Human Fabs

Figure 2. Binding of human monoclonal IgG Fabs to purified mouse α-fodrin brain extract by Western blot analysis. All of the Fabs specifically bound to the 150-kd fragment of cleaved α-fodrin and did not react with 240-kd intact α-fodrin. The human monoclonal anti-Ebola virus Fab ELZ510 was used as a negative control.

transferred to a polyvinylidene difluoride membrane or coated on microtiter wells. After four rounds of biopanning against α-fodrin blotted on a polyvinylidene difluoride membrane, a significant increase in eluted phage was observed, indicating enrichment for antigen-binding Fab-phages. Individual clones, expressed as soluble Fabs by excising the gene III from the pcomb3 phagemid DNA from the last round of selection, were tested for binding to α-fodrin by Western blotting. This analysis yielded 19 Fabs that exhibited strong binding to the 150-kd fragment of cleaved α-fodrin and no binding to intact α-fodrin (240 kd), although present in significant excess, or the 120-kd cleaved form of α-fodrin (Figure 2). The Fabs also failed to react with Western blots of HeLa lysate, which contained intact α-fodrin, but not 120- or 150-kd α-fodrin, as determined by staining with mouse mAb AA6. Sequencing the DNA encoding the heavy chain variable region of the 19 Fabs revealed that 4 Fabs isolated from patient SS23 (SK402, SK415, SK460, and SL420) and 2 Fabs isolated from patient SS30 (RK412 and RK413) were unique, whereas the remaining sequences were repeats of the six sequences (Table 2).

The IgG-Derived Anti-150-kd α-Fodrin Fabs Are Derived as a Result of an Affinity-Matured Antigen-Driven Antibody Response

Next, the variable heavy and light chain genes of the IgG-derived anti-150-kd α-fodrin Fab fragments were compared with the closest germline sequences in the GenBank database (Table 2). The Ab heavy chain is the major contributor to antigen-binding in many instances and so detailed analysis was focused on this chain. All of the variable heavy chain region genes of the anti-150-kd α-fodrin IgG Fabs were highly mutated, and exhibited a high replacement (R) to silent (S) mutation ratio (R/S ratio) for the complementarity determining regions (CDRs) (CDR1 and CDR2) compared to the framework regions (FR) (FR1, FR2, and FR3), characteristic of an affinity-matured antigen-driven Ab response. No particular restriction in the VH or JH gene usage of the anti-150-kd α-fodrin IgG Fabs was observed (Table 2), neither did the analysis reveal any restriction in the germline usage within the context of the VH families used. Unequivocal identification of the closest germline D segment proved impossible because of significant somatic modification.

Epitope Characterization

To pinpoint the epitopes recognized by the anti-150-kd α-fodrin human Fabs, three polypeptides spanning α-fodrin were coated on ELISA wells and tested for reactivity with the Fabs. The polypeptides included JS-1 (1 to 1784 bp), 2.7A (2258 to 4884 bp), and 3'DA (3963 to 7083 bp). None of the tested Fabs recognized any of the peptides, suggesting that the Fabs either recognized regions or partial conformational epitopes of α-fodrin not represented by the peptides.
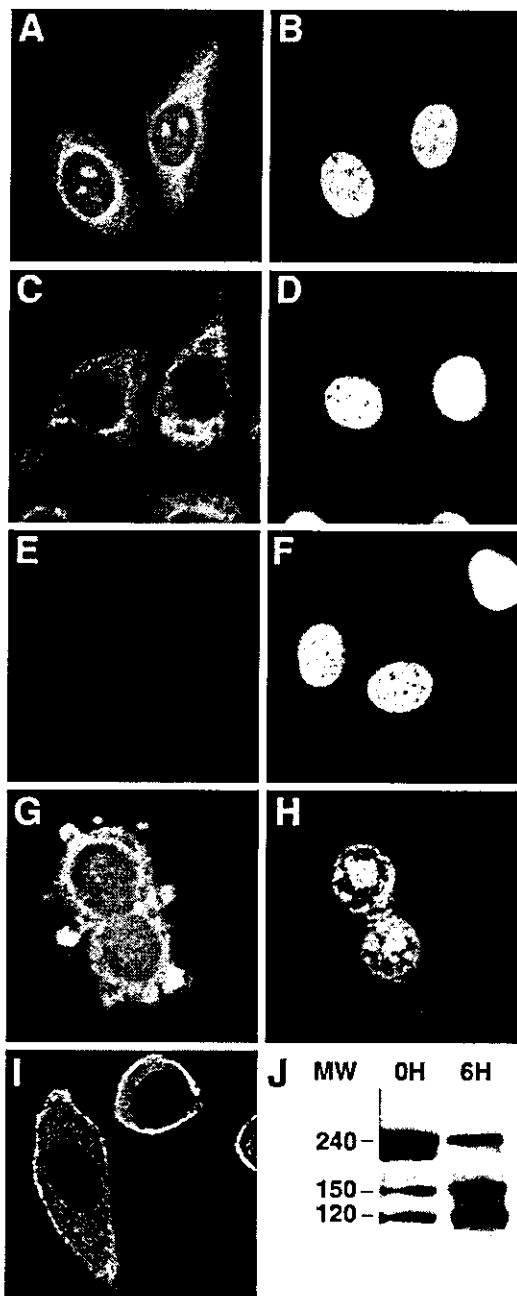
Subcellular Distribution of 150-kd α-Fodrin in HSG Cells

To determine the subcellular distribution of the 150-kd fragment of cleaved α-fodrin, HSG cells were stained with selected human Fabs and examined by laser-scanning confocal microscopy. As shown in Figure 3, Fab SK415 and SK460 exhibited cytoplasmic staining, whereas no staining was observed with a control Fab. Similar cytoplasmic staining was also observed with mouse mAb AA6 recognizing both intact and cleaved α-fodrin (Figure 3I). As previously reported, the cytoplasmic staining of the mouse mAb AA6 was particularly intense, corresponding to the plasma membrane, but this was not observed with the human anti-150-kd α-fodrin Fabs. The fixation method of the HSG cells (ethanol or paraformaldehyde/saponin) did not seem to influence the staining patterns of Fab SK415 and mAb AA6.

Table 2. Deduced Amino Acid Sequences of the Heavy Chain CDR3 Region and Adjacent Framework Regions of Anti-150 kd, α-Fodrin IgGs

Fab	VH/germline	FR3	CDR3	FR4	JH
SK402 (3)	VH1–8	YYCAR	EGWPPTNDY	WGQ	JH4
SK415 (1)	VH3–21	YFCVR	DLCGGRDS	WGQ	JH5
SK460 (2)	VH3–33	YLCAR	EAWHDIGEYDGRRTLGSVPSLDL	WGQ	JH5
SL420 (1)	VH3–21	YYCAR	DGDGYRDY	WGQ	JH4
RK412 (8)	VH1–69	YYCAR	GFGGEDAYYDNFGYYASTEF	WGL	JH3
RK413 (4)	VH4–4	YYCAR	WGPRDLSGRSGGFDP	WGP	JH4

Number in parentheses denotes the number of Fabs that had the same heavy-chain CDR3 sequence. The closest germline gene, VH and JH families for each clone are also shown.

Figure 3. Subcellular distribution of intact and cleaved α-fodrin in human salivary cells. Ethanol-fixed human salivary HSG cells were stained with the human anti-150-kd α-fodrin Fabs SK415 (**A**) and SK460 (**C**), a human anti-HIV-1 gp120 Fab, b12 (**E**, negative control), and the mouse anti-α-fodrin mAb AA6 (**I**). Intense cytoplasmic staining with Fabs SK415 and SK460 and mouse mAb AA6 was observed in the permeabilized cells, although only partial co-localization between the human and mouse mAbs was observed. The cells were also stained with propidium iodine (**B**, **D**, **F**, **H**). Apoptotic HSG cells, exhibiting increased levels of cleaved 120- and 150-kd α-fodrin (**J**, 6H) compared to nonapoptotic cells (**J**, 0H), were also stained with Fab SK415 (**G**) and showed intense staining at the surface blebs.

Cleaved 150-kd α-Fodrin Is Present in Blebs of Apoptotic HSG Cells

Previous studies have shown that α-fodrin is cleaved by different apoptotic enzymes, but the question remained as to how α-fodrin, an intracellular protein, became ex-

posed to the immune system. One possibility is that 150-kd fragments of α-fodrin are exposed on the cell surface during the morphological and biochemical process of apoptosis. Recent reports have demonstrated that certain SS-associated autoantigens, including La, translocate during apoptosis to the cell surface, and particularly to cell surface blebs.[34–36] To determine whether 150-kd α-fodrin fragments become concentrated at the surface of apoptotic HSG cells, apoptosis was induced in HSG cell cultures by tumor necrosis factor-α and cyclo-heximide, and the cells stained with the anti-150-kd α-fodrin Fab SK415 or anti-HIV-1 gp120 Fab (negative control), and propidium iodine (PI). Apoptotic cells were visualized by the binding of fluorescein isothiocyanate-annexin V to phosphatidylserine on the cell surface before fixation and by morphological appearance, including nuclear condensation, surface blebbing, and cell shrinkage (Figure 3, G and H). HSG cell cultures induced by tumor necrosis factor-α and cycloheximide to undergo apoptosis were also analyzed by Western blot and showed increased levels of cleaved 120- and 150-kd α-fodrin (Figure 3J, 6H) compared to noninduced HSG cell cultures, which contained only low amounts of constitutive apoptotic cells, as previously reported (Figure 3J, 0H).[14,17] Confocal analysis demonstrated that anti-150-kd α-fodrin translocated to cell surface blebs of apoptotic HSG cells (Figure 3G). No staining was observed with a control human Fab Ab against HIV-1 gp120 (data not shown).

Localization of 150-kd Cleaved α-Fodrin within SS Salivary Gland Tissue

To determine the distribution of 150-kd fragments of α-fodrin in salivary tissue from patients with active SS, fresh-frozen labial biopsies from three SS patients were obtained and examined by immunohistochemistry. Cryostat tissue sections were stained with anti-150-kd α-fodrin Fab SK415 and a mouse anti-α-fodrin mAb AA6 (Figure 4, A and B). Laser-scanning confocal microscopy of the SS-infiltrated salivary gland using SK415 revealed intense staining of the acinar epithelia cells, with intensification at the cell surface and co-localization with the mouse anti-α-fodrin mAb (Figure 4C, solid arrows). However, SK415 also exhibited intense patchy staining corresponding to the lymphocytic infiltrate immediately surrounding the affected acini, an area not stained by the mAb AA6 or the fluorescein isothiocyanate-labeled anti-human F(ab')₂ Ab alone (Figure 4, open arrows). The SK415 staining in this area was not confined to cells, but seemed to be associated with 150-kd α-fodrin, which had leaked from inflamed glandular cells. The unaffected duct cells were stained by mAb AA6 (Figure 4, arrowheads), but only weakly by Fab SK415. Similarly, duct cells from normal salivary gland tissue were stained by mAb AA6, but not, or only weakly, by Fab SK415 (Figure 4D). The fixation method of the labial biopsy sections (ethanol or acetone) did not seem to influence the staining patterns of Fab SK415 and mAb AA6.
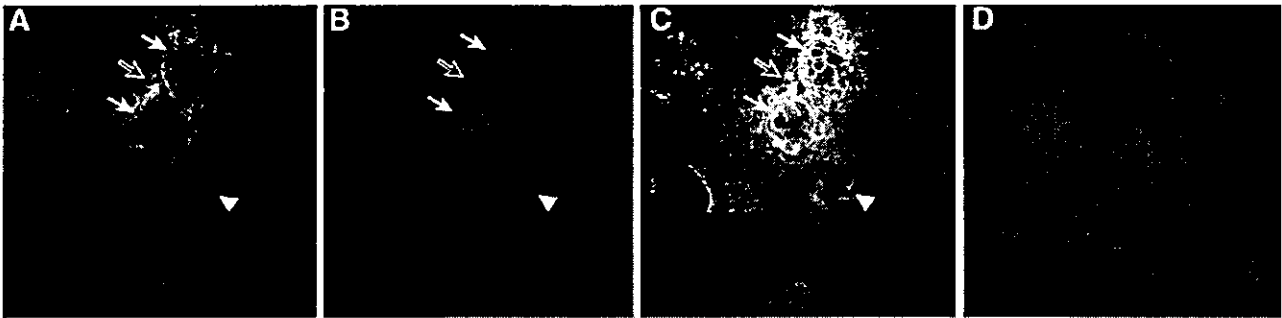
Figure 4. Distribution of cleaved and intact α-fodrin in salivary gland tissue of a SS patient with active disease. Tissue sections from salivary gland biopsies of patients with SS were stained with human anti-150-kd α-fodrin Fab SK415 (A, green) and mouse anti-α-fodrin mAb AA6 (B, red) and analyzed by laser-scanning confocal microscopy. Intense staining corresponding to acinar epithelia cells, and with intensification at the cell surface was observed with SK415 (solid arrows). Only partial co-localization was observed between Fab SK415 and mAb AA6 (C), because Fab SK415, but not mAb AA6, also stained areas corresponding to the lymphocytic infiltrate surrounding the affected acini (open arrow), whereas AA6, but not SK415, stained unaffected ducts (arrowhead). Duct cells from a normal salivary gland were stained with AA6, but not, or only weakly, with SK415 (D). No staining of the salivary gland tissue sections was observed with the negative control Fab b12 or a fluorescein isothiocyanate-labeled anti-human F(ab)₂ alone (not shown).

Discussion

Lymphocyte infiltration in the salivary glands leading to glandular destruction is a common finding in SS patients. The infiltrate consists of predominantly T cells as well as large numbers of B and plasma cells that actively produce immunoglobulin with autoimmune reactivity. To elucidate the components of this immunopathology, we examined the Ab response to α-fodrin in SS patients using serology and phage display cloning.

In the initial study proposing anti-α-fodrin Abs as a disease marker of SS, Western blot analysis of a large panel of Japanese SS patients showed that IgG Ab to 120-kd cleaved α-fodrin could be used as a marker for SS, because it exhibited high sensitivity (95%) and specificity (100%).[7] Subsequently, anti-120-kd α-fodrin Abs were also found in some patients with SLE without SS.[9] The high sensitivity and specificity of anti-α-fodrin Ab as a diagnostic marker of SS has been questioned,[21] although other investigators have also found good correlation between SS and anti-α-fodrin Abs, although the sensitivity was lower than in the Japanese study.[11,37] We investigated a panel of SS patients fulfilling the strict San Diego criteria by evaluating serum panels by both ELISA and Western blotting using purified mouse brain α-fodrin, similar to the antigen source used in the initial Japanese study. This antigen preparation contains both intact (240 kd) and cleaved forms (eg, 120 kd, 150 kd) of α-fodrin, and thus will also be recognized by Abs that specifically bind epitopes accessible only on the cleaved forms of α-fodrin, such as those cloned in this study. Our study demonstrated significant differences in sensitivity between ELISA and Western blotting, suggesting that a major part of the α-fodrin Ab response is directed against conformational epitopes, or that the affinity of the anti-α-fodrin Ab in some SS patients was not sufficient to allow detection by Western blotting. Nearly all (98%) of the SS patients were positive for α-fodrin by ELISA, whereas anti-α-fodrin Ab reactivity by Western blotting was significantly lower (52%), and only 36.0% stained the 120-kd α-fodrin fragment. Some differences in α-fodrin Ab profiles were observed between the American and the Japanese SS patient groups, probably because the two

groups represent two distinct populations with different genetic and environmental influences.

Interestingly, we found that ~25% of both the American and Japanese SS sera recognized a 150-kd fragment of cleaved α-fodrin, an Ab specificity not previously evaluated. This specificity was not seen in a panel of sera from healthy individuals and patients with SLE or RA. Molecular analysis of the anti-150-kd Ab response using IgG Ab phage display libraries generated from two of anti-150-kd seropositive SS patients yielded a panel of hmAbs that specifically recognized the 150-kd form of cleaved α-fodrin and not 120-kd or intact α-fodrin. The specificity of these hmAbs is distinct from that of the currently available mouse anti-α-fodrin mAbs recognizing 150-kd α-fodrin, which also bind 120-kd α-fodrin and intact α-fodrin.

In the NFS/sld SS mouse model, dysregulation of anti-fodrin CD4⁺ T cells leads to Fas-mediated apoptosis of salivary gland epithelial cells and a corresponding increase in clinical symptoms.[8] In humans, a similar scenario has been proposed, and increased apoptosis has been observed in SS salivary glands. Fas expression in the salivary gland cells and FasL on the infiltrating CD4⁺ T cell in SS patients have been reported, although their roles in disease pathology remain to be elucidated.[38] In addition, CTL-mediated lysis/apoptosis though the granzyme and perforin pathways may be involved in salivary gland destruction.[2] In the mouse model,[8] the increased apoptosis was accompanied by an increase in cleaved 120-kd α-fodrin in the affected tissue, as well as in serum anti-120-kd Ab levels, similar to our observation of cleaved 150-kd α-fodrin in SS patients. Indeed, treatment of mice with caspase inhibitors prevented induction of SS,[19] suggesting that α-fodrin cleavage and anti-α-fodrin Ab production is more that an epiphenomenon. We found the 150-kd α-fodrin fragment within affected acinar epithelial cells, and also in the surrounding lymphocytic infiltrate. In the latter areas, the staining was not confined to cells, suggesting leakage of the 150-kd α-fodrin fragment from the apoptotic acinar/ductal epithelial cells into the surrounding interstitium. Interestingly, leakage of 150-kd fragments of α-fodrin has also been observed in tissue cultures of apoptotic human neuroblastoma

cells.[39] In contrast, the anti-150-kd Fabs stained normal salivary cells with lower intensity than a mouse mAb recognizing both intact and cleaved α-fodrin. Our observation seems to support earlier findings that low levels of 120-kd and 150-kd are present in normal cells, but are significantly increased during apoptosis.[14] Our study also suggests that 150-kd α-fodrin is translocated to cell surface blebs in apoptotic HSG cells, similar to Ro/SSA,[35,36] thereby possibly presenting it to the immune system and eliciting an Ab response. Previous studies have shown α-fodrin to be cleaved by calpain in apoptotic T cells, and by calpain and caspases in anti-Fas-stimulated Jurkat cells and/or neuronal apoptosis.[15-17] In human SS, the 150-kd α-fodrin fragments are most likely the result of caspase cleavage,[18,19] but this requires further analysis. In addition, α-fodrin can be cleaved by an unidentified protease present in granules of CD8+ CTLs.[18] Interestingly, membrane blebbing during apoptosis has been suggested to be partially due to fodrin cleavage.[14]

In conclusion, our data supports the theory that in SS patients, α-fodrin is cleaved during apoptosis in the inflamed salivary gland tissue and elicits an Ab response to the cleaved products. Our study also showed that the Ab response to α-fodrin in SS patients is not limited to Abs against the 120-kd fragment, but includes other cleaved products, such as the 150-kd fragment. Inclusion of these Ab specificities would likely increase the sensitivity of the anti-α-fodrin Ab test, and enhance its usefulness as a diagnostic marker of human SS. The isolated human monoclonal Abs to cleaved α-fodrin may serve as useful reagents for diagnostic immunohistochemical analysis of SS salivary gland tissue and study of SS pathogenesis.

References

1. Fox RI, Tornwall J, Maruyama T, Stern M: Evolving concepts of diagnosis, pathogenesis, and therapy of Sjogren's syndrome. Curr Opin Rheumatol 1998, 10:446–456
2. Tapinos NI, Polihronis M, Tzioufas AG, Skopouli FN: Immunopathology of Sjogren's syndrome. Ann Med Interne (Paris) 1998, 149:17–24
3. Jonsson R, Moen K, Vestrheim D, Szodoray P: Current issues in Sjogren's syndrome. Oral Dis 2002, 8:130–140
4. Fox R: Sjögren's Syndrome: Primer on the Rheumatic Diseases. Atlanta, Arthritis Foundation, 1998, pp 283–286
5. Vitali C, Bombardieri S, Moutsopoulos HM, Balestrieri G, Bencivelli W, Bernstein RM, Bjerrum KB, Braga S, Coll J, de Vita S, et al: Preliminary criteria for the classification of Sjogren's syndrome. Results of a prospective concerted action supported by the European Community. Arthritis Rheum 1993, 36:340–347
6. Vitali C, Bombardieri S, Moutsopoulos HM, Coll J, Gerli R, Hatron PY, Kater L, Konttinen YT, Manthorpe R, Meyer O, Mosca M, Ostuni P, Pellerito RA, Pennec Y, Porter SR, Richards A, Sauvezie B, Schiodt M, Sciuto M, Shoenfeld Y, Skopouli FN, Smolen JS, Soromenho F, Tishler M, Wattiaux MJ: Assessment of the European classification criteria for Sjogren's syndrome in a series of clinically defined cases: results of a prospective multicentre study. The European Study Group on Diagnostic Criteria for Sjogren's Syndrome. Ann Rheum Dis 1996, 55:116–121
7. Haneji N, Nakamura T, Takio K, Yanagi K, Higashiyama H, Saito I, Noji S, Sugino H, Hayashi Y: Identification of alpha-fodrin as a candidate autoantigen in primary Sjogren's syndrome. Science 1997, 276:604–607
8. Ishimaru N, Saegusa K, Yanagi K, Haneji N, Saito I, Hayashi Y: Estrogen deficiency accelerates autoimmune exocrinopathy in murine Sjogren's syndrome through Fas-mediated apoptosis. Am J Pathol 1999, 155:173–181
9. Watanabe T, Tsuchida T, Kanda N, Mori K, Hayashi Y, Tamaki K: Anti-alpha-fodrin antibodies in Sjogren syndrome and lupus erythematosus. Arch Dermatol 1999, 135:535–539
10. Miyagawa S, Yanagi K, Yoshioka A, Kidoguchi K, Shirai T, Hayashi Y: Neonatal lupus erythematosus: maternal IgG antibodies bind to a recombinant NH2-terminal fusion protein encoded by human alpha-fodrin cDNA. J Invest Dermatol 1998, 111:1189–1192
11. Witte T, Matthias T, Oppermann M, Helmke K, Peter HH, Schmidt RE, Tishler M: Prevalence of antibodies against alpha-fodrin in Sjogren's syndrome: comparison of 2 sets of classification criteria. J Rheumatol 2003, 30:2157–2159
12. Perrin D, Aunis D: Reorganization of alpha-fodrin induced by stimulation in secretory cells. Nature 1985, 315:589–592
13. Leto TL, Pleasic S, Forget BG, Benz Jr EJ, Marchesi VT: Characterization of the calmodulin-binding site of nonerythroid alpha-spectrin. Recombinant protein and model peptide studies. J Biol Chem 1989, 264:5826–5830
14. Martin SJ, O'Brien GA, Nishioka WK, McGahon AJ, Mahboubi A, Saido TC, Green DR: Proteolysis of fodrin (non-erythroid spectrin) during apoptosis. J Biol Chem 1995, 270:6425–6428
15. Martin SJ, Finucane DM, Amarante-Mendes GP, O'Brien GA, Green DR: Phosphatidylserine externalization during CD95-induced apoptosis of cells and cytoplasts requires ICE/CED-3 protease activity. J Biol Chem 1996, 271:28753–28756
16. Vanags DM, Porn-Ares MI, Coppola S, Burgess DH, Orrenius S: Protease involvement in fodrin cleavage and phosphatidylserine exposure in apoptosis. J Biol Chem 1996, 271:31075–31085
17. Nath R, Raser KJ, Stafford D, Hajimohammadreza I, Posner A, Allen H, Talanian RV, Yuen P, Gilbertsen RB, Wang KK: Non-erythroid alpha-spectrin breakdown by calpain and interleukin 1 beta-converting-enzyme-like protease(s) in apoptotic cells: contributory roles of both protease families in neuronal apoptosis. Biochem J 1996, 319:683–690
18. Nagaraju K, Cox A, Casciola-Rosen L, Rosen A: Novel fragments of the Sjogren's syndrome autoantigens alpha-fodrin and type 3 muscarinic acetylcholine receptor generated during cytotoxic lymphocyte granule-induced cell death. Arthritis Rheum 2001, 44:2376–2386
19. Saegusa K, Ishimaru N, Yanagi K, Mishima K, Arakaki R, Suda T, Saito I, Hayashi Y: Prevention and induction of autoimmune exocrinopathy is dependent on pathogenic autoantigen cleavage in murine Sjogren's syndrome. J Immunol 2002, 169:1050–1057
20. Maeno N, Takei S, Imanaka H, Oda H, Yanagi K, Hayashi Y, Miyata K: Anti-alpha-fodrin antibodies in Sjogren's syndrome in children. J Rheumatol 2001, 28:860–864
21. Witte T, Matthias T, Arnett FC, Peter HH, Hartung K, Sachse C, Wigand R, Braner A, Kalden JR, Lakomek HJ, Schmidt RE: IgA and IgG autoantibodies against alpha-fodrin as markers for Sjogren's syndrome. Systemic lupus erythematosus. J Rheumatol 2000, 27:2617–2620
22. Yanagi K, Ishimaru N, Haneji N, Saegusa K, Saito I, Hayashi Y: Anti-120-kDa alpha-fodrin immune response with Th1-cytokine profile in the NOD mouse model of Sjogren's syndrome. Eur J Immunol 1998, 28:3336–3345
23. Fox RI, Saito I: Criteria for diagnosis of Sjögren's syndrome. Rheum Dis Clin North Am 1994, 20:391–407
24. Cheney R, Levine J, Willard M: Purification of fodrin from mammalian brain. Methods Enzymol 1986, 134:42–54
25. Janicke RU, Ng P, Sprengart ML, Porter AG: Caspase-3 is required for alpha-fodrin cleavage but dispensable for cleavage of other death substrates in apoptosis. J Biol Chem 1998, 273:15540–15545
26. Chomczynski P, Sacchi N: Single-step method of RNA isolation by acid guanidinium thiocyanate-phenol-chloroform extraction. Anal Biochem 1987, 162:156–159
27. Persson MA, Caothien RH, Burton DR: Generation of diverse high-affinity human monoclonal antibodies by repertoire cloning. Proc Natl Acad Sci USA 1991, 88:2432–2436
28. Barbas III CF, Wagner J: Synthetic human antibodies selecting and evolving functional protein. Methods CTMIE 1995, 8:94–103
29. Burton DR, Barbas III CF, Persson MA, Koenig S, Chanock RM, Lerner RA: A large array of human monoclonal antibodies to type 1 human immunodeficiency virus from combinatorial libraries of asymptomatic seropositive individuals. Proc Natl Acad Sci USA 1991, 88:10134–10137

30. Maruyama T, Rodriguez LL, Jahrling PB, Sanchez A, Khan AS, Nichol ST, Peters CJ, Parren PW, Burton DR: Ebola virus can be effectively neutralized by antibody produced in natural human infection. J Virol 1999, 73:6024–6030

31. Warmerdam PA, van den Herik-Oudijk IE, Parren PW, Westerdaal NA, van de Winkel JG, Capel PJ: Interaction of a human Fc gamma RIIb1 (CD32) isoform with murine and human IgG subclasses. Int Immunol 1993, 5:239–247

32. Ditzel HJ, Binley JM, Moore JP, Sodroski J, Sullivan N, Sawyer LS, Hendry RM, Yang WP, Barbas III CF, Burton DR: Neutralizing recombinant human antibodies to a conformational V2- and CD4-binding site-sensitive epitope of HIV-1 gp120 isolated by using an epitope-masking procedure. J Immunol 1995, 154:893–906

33. Binley JM, Ditzel HJ, Barbas III CF, Sullivan N, Sodroski J, Parren PW, Burton DR: Human antibody responses to HIV type 1 glycoprotein 41 cloned in phage display libraries suggest three major epitopes are recognized and give evidence for conserved antibody motifs in antigen binding. AIDS Res Hum Retroviruses 1996, 12:911–924

34. Casciola-Rosen LA, Anhalt G, Rosen A: Autoantigens targeted in systemic lupus erythematosus are clustered in two populations of surface structures on apoptotic keratinocytes. J Exp Med 1994, 179:1317–1330

35. Baboonian C, Venables PJ, Booth J, Williams DG, Roffe LM, Maini RN: Virus infection induces redistribution and membrane localization of the nuclear antigen La (SS-B): a possible mechanism for autoimmunity. Clin Exp Immunol 1989, 78:454–459

36. Bachmann M, Chang S, Stor H, Kukulies J, Muller WE: Shuttling of the autoantigen La between nucleus and cell surface after UV irradiation of human keratinocytes. Exp Cell Res 1990, 191:171–180

37. Zandbelt M, Degen W, van de Putte L, van Venrooij W, van den Hoogen Nijmegen F: Anti-a-fodrin antibodies: not specific nor sensitive for Sjögren's syndrome. Arthritis Rheum 1999, 42(Abstract 428 Suppl):S142

38. Kong L, Ogawa N, Nakabayashi T, Liu GT, D'Souza E, McGuff HS, Guerrero D, Talal N, Dang H: Fas and Fas ligand expression in the salivary glands of patients with primary Sjogren's syndrome. Arthritis Rheum 1997, 40:87–97

39. Dutta S, Chiu YC, Probert AW, Wang KK: Selective release of calpain produced alphaII-spectrin (alpha-fodrin) breakdown products by acute neuronal cell death. Biol Chem 2002, 383:785–791

Activation of Epstein–Barr virus by saliva from Sjogren's syndrome patients

YOSHIFUMI NAGATA,* HIROKO INOUE,* KOICHI YAMADA,* HIROYUKI HIGASHIYAMA,* KENJI MISHIMA,* YASUHIRO KIZU,† IENAKA TAKEDA,† FUMIO MIZUNO,‡ YOSHIO HAYASHI§ & ICHIRO SAITO* *Department of Pathology, Tsurumi University School of Dental Medicine, Yokohama, Japan, †Department of Oral Medicine, Tokyo Dental College, Chiba, Japan, ‡Department of Microbiology, Tokyo Medical University, Tokyo, Japan, and §Department of Pathology, Tokushima University School of Dentistry, Tokushima, Japan

SUMMARY

The aim of this study was to examine the mechanism of Epstein–Barr virus (EBV) activation by soluble factors from the inflamed salivary glands of patients with Sjogren's syndrome (SS). Saliva from SS patients was used to examine the regulation of EBV activation by an inflammatory salivary microenvironment. Transient transfection of the EBV-negative salivary gland cell line (HSY) with BZLF1, a *trans*-activating EBV gene promoter-fusion construct (Zp-luc), was used in this study. The results showed that under conditions where the BZLF1 promoter is activated by potent stimuli, SS saliva (from eight of 12 patients) exerts a significant effect on expression of the luciferase gene. A specific inhibitor of protein kinase C did not affect the SS saliva-induced Zp-luc activity, whereas treatment with inhibitors of calmodulin, calcineurin and IP_3, dose-dependently decreased this induction. Transforming growth factor $\beta 1$ (TGF-$\beta 1$), which is known to be expressed in SS salivary glands, dose-dependently induced Zp-luc activity. Hence, these results demonstrate the activation of EBV by SS saliva and suggest that EBV activation at the inflammatory site may occur in the presence of TGF-$\beta 1$ via triggering of the mitogen-activated protein kinase (MAPK) kinase signalling pathway.

INTRODUCTION

Sjogren's syndrome (SS) is an organ-specific disorder affecting the salivary and lacrimal glands and leads to clinical symptoms of dryness of the mouth and eyes. Although the pathogenesis of SS remains unclear, there is reportedly a high incidence of Epstein–Barr virus (EBV) reactivation in SS, contributing to the initiation or perpetuation of an immune response in target organs. EBV antigens and EBV DNA have been found in infiltrating lymphocytes and salivary gland epithelial cells of

SS patients.[1,2] Infectious EBV is present in both the saliva of SS patients[3–5] and culture supernatants of cell lines established from SS patients.[6] Other defined manifestations of an active EBV infection are the presence of infected B cells that can transform into B-cell lymphomas in the circulation.[7] Mariette *et al.* previously used *in situ* hybridization to detect EBV DNA in a substantial proportion of lymphoid cells and epithelial cells in salivary glands from patients with SS.[2] It has also been shown that antibodies against EBV antigens are elevated in SS sera.[8,9] Furthermore, we have recently reported an increase in the enzymatic activity of apoptotic protease, by EBV activation, to be involved in the proteolysis of 120 000 molecular weight (MW) α-fodrin autoantigen during the development of SS.[10,11] As EBV is known to induce strong immune responses,[12,13] these reports suggest that a reactivated EBV infection may play a role in SS.

EBV is a widely occurring virus of the herpes family that infects epithelial cells of the salivary glands and oropharyngeal tissue, as well as B cells. After the primary infection, the virus remains latent in the host and occasionally becomes reactivated. Reactivation of EBV requires replication of viral genes and transcriptional induction of immediate-early genes mediated by expression of the BZLF1 gene. The BZLF1 gene product, ZEBRA, is considered to first be transcribed in association

with viral replication and to be indispensable for the reactivation of EBV.[14,15] Expression of the BZLF1 gene that encodes ZEBRA has been reported to be induced by 12-O-tetradecanoylphorbol-13-acetate (TPA),[16] the calcium ionophore A23187,[17] cross-linking of cell-surface immunoglobulin G (IgG),[18] n-butyrate,[19] the formation of het DNA associated with P3HR-1 super-infection,[20,21] nitric oxide (NO) inhibitor,[22] human herpesvirus 6 (HHV6) superinfection *in vitro*[23] and transforming growth factor-β1 (TGF-β1).[24] However, the physiological stimuli responsible for the EBV activation in SS have not been characterized.

Moreover, how reactivation of EBV is actually induced in lesions associated with SS, and which signalling pathways are involved in the process of viral reactivation, have not yet been clarified. To elucidate the mechanism underlying the EBV reactivation involved in the pathogenesis and progression of SS, we analysed the contribution of EBV activation by soluble factors in inflammatory saliva using a BZLF1 promoter fusion construct (Zp-luc) transfected into the human salivary gland cell line, HSY, and investigated the signalling pathways that might be involved in EBV reactivation in SS.

MATERIALS AND METHODS

Saliva samples

Saliva samples were collected from 12 patients with primary SS. All patients were seen at the Ichikawa General Hospital of Tokyo Dental College, and diagnosed according to the criteria of Fox & Saito.[25] These patients had not received glucocorticoids or immunosuppressive agents for at least 6 months prior to saliva collection.

All of the patients were women (mean age: 56 years). As age-matched controls, saliva samples were also obtained from 10 women who had no clinical evidence of systemic autoimmune disease. The samples were centrifuged at 12 000 *g* for 45 min and filtered through a 0·22-μm filter to remove cells, virus and particulate debris; aliquots were stored at −80°.

Cell culture, transfections and chemicals

The salivary gland epithelial cell line HSY[26] (kindly provided by Dr M. Sato of Tokushima University) was cultured at 37° in minimal essential medium (MEM) containing HEPES (10 mM), penicillin (100 IU/ml), streptomycin (100 μg/ml), and 10% fetal calf serum (FCS). The EBV-positive B-cell line, B95-8, was maintained in RPMI-1640 supplemented with penicillin (100 IU/ml), streptomycin (100 μg/ml) and 10% FCS at 37° in a humidified atmosphere of 5% CO_2 in air. We used polymerase chain reaction (PCR) techniques to generate a derivative of a BZLF1 promoter (Zp) construct. The following forward and reverse oligomers were used as primers to create the promoter of the BZLF1 gene, respectively: 5′-CTGCAGCCATGCATATTT-CAACTGGG-3′ and 5′-GTCGACGCAAGGTGCAATGTTTA-GTG-3. The PCR-amplified promoter fragments, including the *KpnI/SalI* sites were cloned into the multiple cloning site of the pGL3-basic vector (Promega, Madison, WI), upstream from the luciferase gene. The Zp-luciferase gene (Zp-luc) was transfected into HSY cells using Lipofectin (Life Technologies, Grand Island, NY). The vector pGL3-basic (lacking a promoter) and the vector pGL3-control (Promega) served as negative and

positive controls, respectively. Briefly, the transfection medium containing 2 μg of plasmid DNA and 20 μl of Lipofectin reagent in 200 μl of serum-free Dulbecco's modified Eagle's minimal essential medium (DMEM) was incubated for 20 min at room temperature and then diluted with serum-free DMEM to a final volume of 2 ml and added to HSY cells, plated the previous day. The transfection process occurred at 37° for 5 hr after which the DNA-containing medium was replaced with 2 ml of DMEM containing 10% FCS. TPA, calcium ionophore A23187, compound R24571 (calmodulin inhibitor), wortmaninn (IP_3-kinase inhibitor), cyclosporin A (calcineurin inhibitor), and 1-(5-isoquinolinyl sulphonyl)-2-methylpiperazine (H-7) [a protein kinase C (PKC) inhibitor] were purchased from Sigma Co. (St Louis, MO); and U0126 [a mitogen-activated protein kinase (MAPK) inhibitor] was purchased from Promega.

Luciferase assay

In order to test the Zp response to various stimuli, we used a plasmid carrying a region of Zp from −221 to +12 bp, which was cloned upstream of the coding sequence of the bacterial luciferase gene (Zp-luc). The Zp region was previously reported to contain TPA response elements. Zp-luc was transfected into the EBV-negative salivary gland cell line, HSY, which was treated with stimuli and assayed for luciferase activity. The transfected cells were incubated for 24 hr followed by stimulation with a 1 : 50 volume of saliva. TGF-β1 (Genzyme Corp., Cambridge, MA) was added to the transfected cells under the same conditions. After rinsing with phosphate-buffered saline (PBS), cells were lysed with reporter lysis buffer (Promega) and the cell lysate was analysed by the luciferase assay with the Promega kit in a Lumat (Bio-Rad, Hercules, CA). To control transfection efficiency, plasmid pRL-TK (Promega) was co-transfected with the luciferase reporter constructs at a ratio of 1 : 4. The results showed the difference in the relative efficiency of transfection between constructs to be negligible. For the assay in the presence of TPA or A23187, cells were also treated with these chemicals after transfection. The inducibility of luciferase activity was defined as the fold activity of the sample to the untreated control. Data shown are from a representative experiment carried out a minimum of three times.

Quantification of TGF-β1 in saliva by enzyme-linked immunosorbent assay

TGF-β1 concentrations in saliva were measured using the Quantikine enzyme-linked immunosorbent assay (ELISA) kit (R & D, Minneapolis, MN). Briefly, saliva was used immediately after thawing from −80° and latent TGF-β1 was activated to immunoreactive TGF-β1. Diluted saliva samples were placed in a 96-well microtitre plate, previously coated with recombinant human TGF-β1 soluble receptor Type II (sRII). After incubation and washing, a horseradish peroxidase-conjugated secondary antibody was added. Hydrogen peroxidase and chromogen were added and colour development was measured at 450 nm using a microplate reader.

Western blot analysis

Cells were harvested, washed briefly with PBS, resuspended in buffer comprising 100 mM Tris–HCl (pH 7·6), 50 mM NaCl, 2 mM EDTA 0·5% Nonidet P-40 (NP-40), 100 μg/ml

phenylmethanesulphonyl fluoride and 1 µg/ml of each of leu-peptin, pepstatin and aprotinin, and then sonicated; protein concentrations were determined using a modified Lowry assay (Bio-Rad). Equal amounts of protein in loading buffer, heated for 5 min at 100° and separated by sodium dodecyl sulphate-polyacrylamide gel electrophoresis (SDS–PAGE) on a 10% gel, were transferred (by electroblotting) to a nitrocellulose membrane. The membrane was stained with Ponceau S sodium salt to verify that the same amount of protein had been deposited in each lane. Anti-ZEBRA monoclonal antibody (mAb) (Dako, Carpinteria, CA) was used as a primary antibody, and horseradish peroxidase-conjugated anti-mouse IgG was used as the secondary antibody. The intensity of ZEBRA bands was measured by densitometric analysis using a colour scanner and NIH image 1.6.2. The amount of ZEBRA induced by TPA (25 ng/ml), TGF-β1 (5 ng/ml), and saliva from SS or normal individuals (1 : 50 vol/vol), with or without neutralizing anti-TGF-β1 antibody (Genzyme Corp.), was expressed as follows: [percentage of the relative amount to the negative control (TPA, TGF-β1, saliva from SS or normal individuals) ÷ (untreated)] × 100.

RESULTS

Activation of the BZLF1 promoter (Zp) in salivary gland cells

The Zp region has previously been reported to be TPA or A23187 responsive in HeLa cells and B cells.[17,27,28] In order to test the Zp activity in salivary glands, we used a plasmid carrying a Zp region (−221 to +12 bp)[28] that was cloned into an upstream portion of the luciferase gene (Zp-luc). Zp-luc was transfected into the salivary gland cell line, HSY, which had been treated with TPA or A23187, and a luciferase assay was performed. As shown in Fig. 1, luciferase activity was dose-dependently induced with TPA and A23187, even in the absence of other EBV genes. We found that this region was also responsive to TPA or A23187 in salivary gland epithelial cells.

Activation of Zp by saliva from SS patients

We next investigated whether some soluble factors are involved in the EBV reactivation that occurs in the microenvironment of SS. We collected saliva samples from 12 SS patients and 10 normal subjects, to reproduce the oral environment. As shown in Fig. 2, eight of the 12 saliva samples from SS patients showed increased luciferase activity. In contrast, luciferase activity was not increased in the normal saliva samples. These findings suggest that some humoral factors in SS saliva might play a major role in the reactivation of EBV, which in turn leads to the progression of SS.

Effects of PKC inhibitors, calcium/calmodulin-dependent protein kinase, and MAPK kinase on Zp activation by SS saliva

In B cells, the mechanism of EBV reactivation has been analysed and reported,[29,30] but the physiological signalling for EBV reactivation in SS has not been characterized. To analyse the signalling pathways occurring downstream of SS
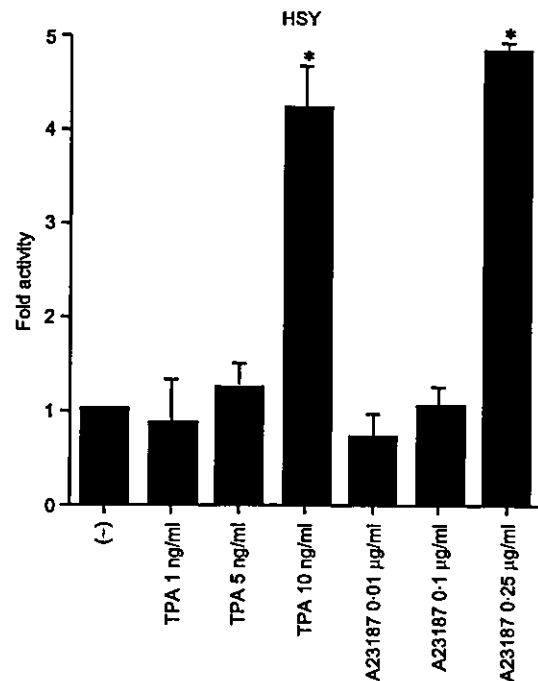

Figure 1. Activation of Zp-luc by 12-*O*-tetradecanoylphorbol-13-acetate (TPA) and A23187 in the Epstein–Barr virus (EBV)-negative salivary gland cell line, HSY. The cells were treated with either TPA (1, 5, or 10 ng/ml) or A23187 (0·01, 0·1, or 0·25 µg/ml), or given no treatment (−). After incubation for 24 hr, the cells were harvested, and luciferase activity was assayed. The bar graph illustrates fold activity. *$P < 0·05$; Mann–Whitney U-test. The error bars represent standard deviation.
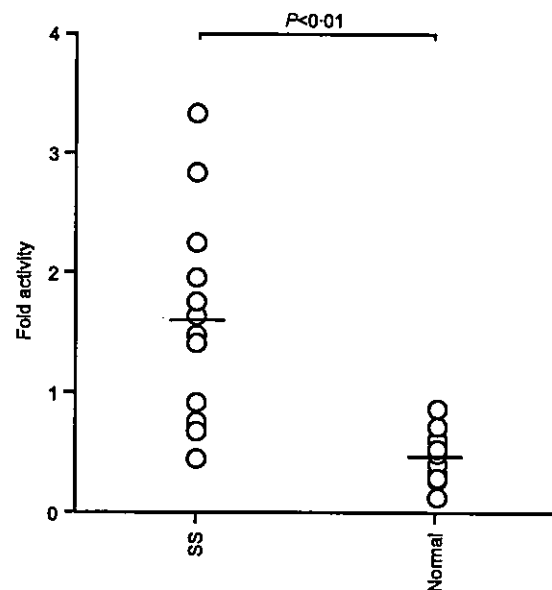

Figure 2. Measurement of luciferase activity in HSY cells transfected with Zp-luc and treated with saliva from the 12 Sjogren's syndrome patients (SS) or 10 normal controls (Normal). $P < 0·01$; Mann–Whitney U-test.

saliva stimulation, in our models of SS we further examined whether Zp-luc activation induced by SS saliva could be inhibited by PKC, calcium/calmodulin-dependent protein kinase or MAPK inhibitors. As shown in Fig. 3a, the PKC inhibitor did not affect luciferase activity, but the inhibitors of IP$_3$ (Fig. 3b), calmodulin (Fig. 3c) and calcineurin (Fig. 3d) decreased Zp-luc activity. The SS saliva used was that with the highest fold activity of Zp-luc shown in Fig. 2.

Moreover, a specific inhibitor of MAPK also reduced Zp-luc activity (Fig. 3e), suggesting that the effects of SS saliva on BZLF1 expression require calcium/calmodulin and the MAPK pathway.

Zp activation by TGF-β1

Finally, we assumed that cytokines, which are expressed in SS, might play a role in the reactivation of EBV. It is known that (in contrast to normal salivary glands) SS salivary glands express increased levels of cytokines,[31,32] but the relationship between these cytokines and EBV reactivation is not well characterized. TGF-β1, which is known to be expressed in SS, can further induce EBV reactivation in the EBV-positive B-cell lines P3HR-1, Akata[24] and B95-8.[33] To investigate cytokine efficiency in Zp activation, we conducted a luciferase assay using TGF-β1. The result indicated that 1 ng/ml of TGF-β1 increases Zp-luc activity (Fig. 4a). Next, to address the issue of the presence of TGF-β1 in saliva, we measured TGF-β1 levels
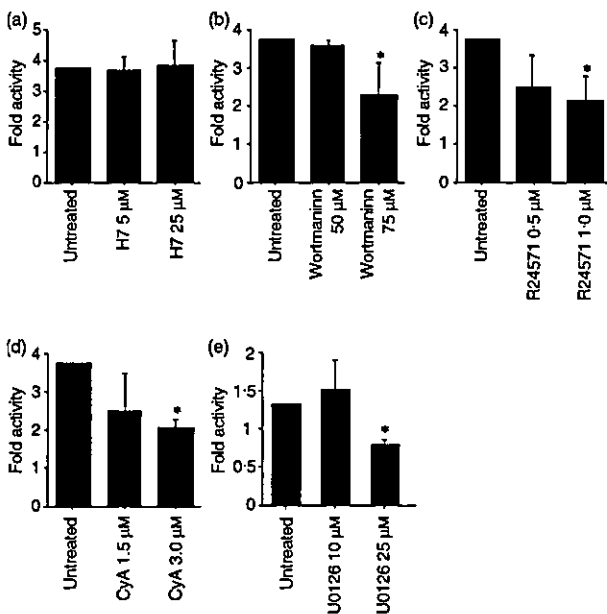

Figure 3. Effects of a protein kinase inhibitor, calmodulin antagonists, and a MAPK kinase (MEK) inhibitor on Sjogren's syndrome (SS) saliva-induced Zp-luc activation. HSY cells were pretreated for 1 hr with H7 (a), Wortmaninn (b), R24571 (c), cyclosporin A (d), or U0126 (e) before the addition of SS saliva. Cells were harvested 24 hr later, and the cell extracts were assayed for luciferase activity. This result is representative of three independent experiments. *P < 0·05; Mann–Whitney U-test.
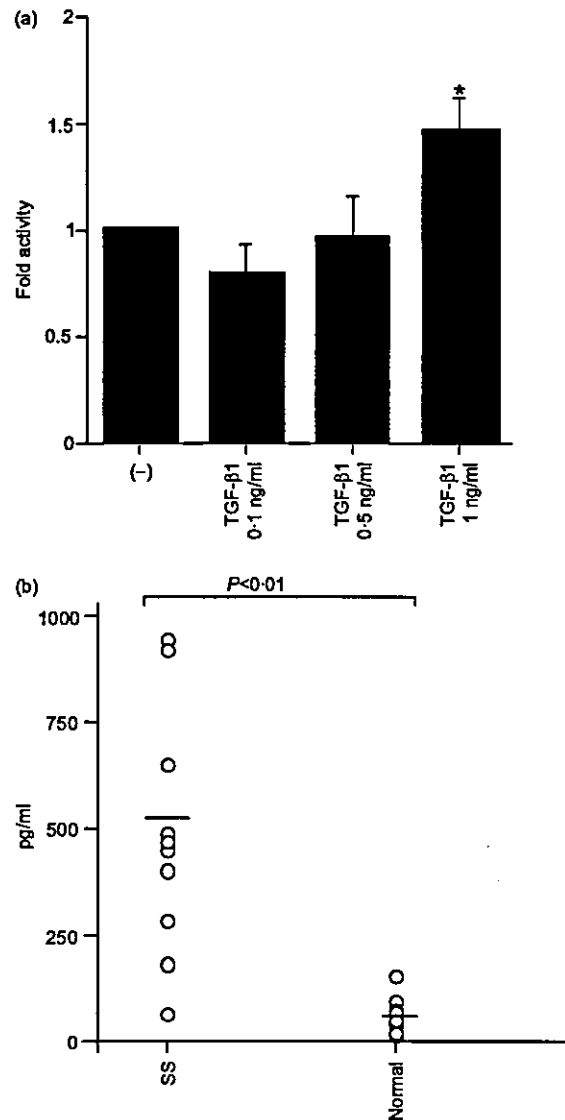
Figure 4. Effect of transforming growth factor-β1 (TGF-β1) on Zp activation. Luciferase assay of the BZLF1 promoter activities in HSY cells stimulated with TGF-β1 after transfection. Cells were harvested 24 hr later, and the cell extracts were assayed for luciferase activity. *P < 0·05; Mann–Whitney U-test (a). TGF-β1 concentrations in saliva were measured by enzyme-linked immunosorbet assay (ELISA) (b). Saliva was used immediately after thawing from −80°. The treated samples were measured at 450 nm using a microplate reader.

using an ELISA. Figure 4(b) shows TGF-β1 concentrations to be significantly elevated in SS saliva compared with the saliva of healthy volunteers. A significant correlation was observed between the level of fold activity and the concentration of TGF-β1 in each saliva sample from SS patients (r = 0·75, P < 0·01). A concentration of 1 ng/ml TGF-β1, higher than the highest concentration in SS saliva, had 1·4-fold Zp-luc activity, whereas the SS saliva stimulated Zp-luc activity by 3·5-fold. These results demonstrate that TGF-β1 alone is not sufficient to stimulate Zp-luc, suggesting the possibility of a synergistic additional factor(s) in SS saliva. We speculate that TGF-β1
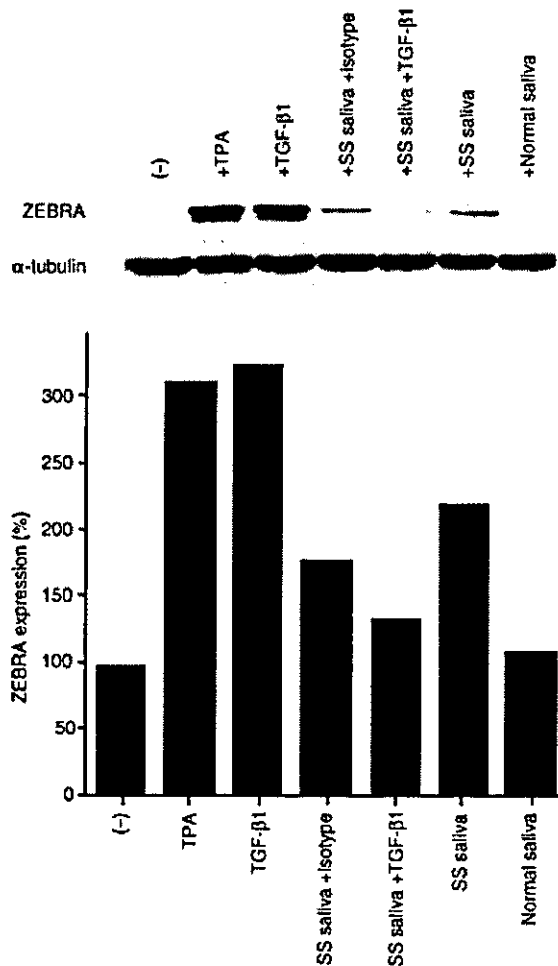
Figure 5. Effect of Sjogren's syndrome (SS) saliva on the expression of ZEBRA in Epstein–Barr virus (EBV)-positive B95-8 cells. B95-8 cells were treated for 48 hr with 25 ng/ml of 12-*O*-tetradecanoylphorbol-13-acetate (TPA) or 5 ng/ml of transforming growth factor-β1 (TGF-β1), or cells were cultured with SS saliva and a normal control for 48 hr. The neutralizing anti-TGF-β1 (10 µg/ml) was added at the start of the culture. ZEBRA bands were quantified by densitometric analysis. The results were calculated and the amount of ZEBRA was expressed as described in the Materials and methods. Tubulin was used for normalizing the amount of protein loaded. The results shown are representative of three independent experiments.

is not the sole activation factor, but a major factor of ZEBRA expression by SS saliva because TGF-β1-specific antibody inhibited the expression of ZEBRA in SS saliva, as shown by Western blotting.

Furthermore, to investigate the effect of SS saliva on expression of ZEBRA protein, we used EBV-positive B95-8 cells in which ZEBRA protein can be induced under several conditions (i.e. by TPA and TGF-β1). B95-8 cells were exposed to SS saliva, which had a high TGF-β1 concentration of 920 pg/ml. As shown in Fig. 5, ZEBRA protein was detected following treatment with SS saliva, suggesting that SS saliva contains factors that induce EBV reactivation. Neutralizing anti-TGF-β1 inhibited the induction of ZEBRA by SS saliva, in contrast to isotype-matched control antibody (Fig. 5). These results sug-

gest that TGF-β1 may play a role in the EBV reactivation of a subpopulation in SS.

DISCUSSION

In the pathogenesis of SS, a role for EBV reactivation has been suggested.[1–4,6] EBV is a ubiquitous human herpesvirus that replicates in the salivary glands during primary infection[34] and the virus remains latent at this site in normal adults.[35] Initiation of the EBV lytic cycle is dependent on transcription of the BZLF1 gene. Although the viral lytic cycle can be induced by various reagents *in vitro*, including TPA,[16] calcium ionophore,[17] anti-IgG,[18] n-butyrate[19] and NO inhibitor,[22] it remains unclear how EBV reactivation is induced in SS. In this study, in order to clarify the association of EBV reactivation in SS pathogenesis and further analyse the mechanism of EBV reactivation, we modelled the reactivation of EBV, which latently infected the salivary gland, using plasmid DNA containing the BZLF1 promoter upstream from the luciferase reporter gene.

The Zp-luc(−221) reporter system has been widely used as a marker of EBV reactivation, even in EBV-negative cells.[36] However, it is well known that the induction of promoter activity by TPA, or TGF-β1, in EBV-negative cells is relatively low.[33,36] These results might be largely a result of the absence of ZEBRA in these assay systems. Regulation of ZEBRA is known to be achieved by two steps.[27] Initial activation of the BZLF1 promoter is weak, but this level of ZEBRA sufficiently induces full activation of the promoter by means of self-promoter bindings. Therefore, the weak fold-induction of Zp-luc seen in our system might correspond to the initial 'weak' activations prior to the occurrence of full activation.

We demonstrated the EBV reactivation model in SS and found that expression of the BZLF1 gene in glandular epithelial cells might be induced via MAPK and calcium/calmodulin dependent-kinase pathways, as previously demonstrated in B lymphocytes.[29,30] However, the physiological stimuli responsible for the EBV activation in SS have not yet been characterized.

Our results showed that treatment with saliva from SS patients increases the reactivation ability of EBV as compared with normal saliva samples. This suggests the existence of factors that are able to induce the reactivation of EBV. It has been reported that infectious EBV is present in the saliva of SS patients[1] and in HHV6 superinfection *in vitro*,[23] but we considered that these viruses were not present in the saliva samples used in the present study, as a result of the saliva processing technique used (centrifugation for 45 min at 12 000 *g* to remove cells and particulate debris, followed by filtering through a 0·22-µm filter). We thus assumed that some soluble factors play a major role in the reactivation of EBV.

The expression of ZEBRA can be accomplished, *in vitro*, by treatment of latent EBV-positive B cells with various activating agents, including TGF-β1, TPA, butyrate, calcium ionophores and anti-IgG. These treatments trigger a variety of cellular signalling pathways, resulting in the activation of cellular transcription factors stimulating transcription from the BZLF1 promoter, Zp.[27,30,37,38] Zp can be activated through PKC and calcium/calmodulin-dependent protein kinase directly cross-linking via anti-IgG.[39] Anti-IgG also induced rapid phosphorylation of MAPK in Akata cells.[30] Moreover, MAPK was

involved in the activation of BZLF1 induced by TGF-β1 in Raji and B95-8 cells.[33] In P3HR-1 and Rael cells, however, MAPK was not involved in the activation of Zp-luc by TGF-β1.[40] This discrepancy might be explained by different characteristics of cell lineage. The signal transduction of Zp-luc activation in salivary gland cells has not been reported. We investigated the SS saliva signal in EBV reactivation in our models by using specific inhibitors of intracellular signals. A specific inhibitor of PKC did not affect the SS saliva-induced Zp-luc activity, whereas treatment with inhibitors of calmodulin, calcineurin, IP$_3$ and MAPK, dose dependently decreased this induction. This implies that the effect of SS saliva on BZLF1 expression requires calcium/calmodulin and/or the MAPK pathway.

TGF-β1 has been shown to exert its effects through a wide range of intracellular routes. Recent studies from several laboratories have reported that Smads are intermediate effector proteins which transduce the TGF-β1 signal from the plasma membrane to the nucleus.[41] TGF-β1 can induce gene expression via c-Jun N-terminal kinase (JNK) activation[42,43] or p38 MAPK.[44] The role of MAPK/ERK in the TGF-β1 signalling pathway has been described.[45] PKC has also been shown to be involved in TPA- and anti-IgG-induced EBV reactivation[30,46] and could play an important role in the signal transduction by TGF-β1.[47,48] This suggests that SS saliva might contain some soluble factor(s), such as TGF-β1, which can induce virus reactivation.

It is known that, in contrast to normal salivary glands, SS salivary glands express increased levels of cytokines.[31,49] Furthermore, recent reports have suggested that in latently infected B cells, the lytic cycle can be induced by TGF-β1[24] and that salivary TGF-β1 concentrations are elevated in SS.[31] In our experiments, TGF-β1 increased Zp-luc activity, and TGF-β1 concentrations were significantly elevated in SS saliva as compared to saliva from healthy volunteers (Fig. 4). Furthermore, we investigated the effect of SS saliva on Zp activation in B cells by Western blot analysis, using an SS saliva sample with a high concentration of TGF-β1. ZEBRA was detected upon exposure to SS saliva (Fig. 5), suggesting that SS saliva contains factors which induce viral reactivation. As shown in Fig. 5, neutralizing anti-TGF-β1 inhibited ZEBRA induction by SS saliva. In SS saliva, TGF-β1 may play a major role in viral reactivation.

In conclusion, we have shown that SS saliva induces Zp-luc activity and that calcium/calmodulin and/or the MAPK pathway is required for this induction, as demonstrated through the use of specific signalling inhibitors. These findings may be of importance for developing new strategies to inhibit EBV reactivation in SS.

ACKNOWLEDGMENTS

REFERENCES

1 Saito I, Servenius B, Compton T, Fox RI. Detection of Epstein–Barr virus DNA by polymerase chain reaction in blood and tissue biopsies from patients with Sjogren's syndrome. J Exp Med 1989; **169:** 2191–8.

2 Mariette X, Gozlan J, Clerc D, Bisson M, Morinet F. Detection of Epstein–Barr virus DNA by *in situ* hybridization and polymerase chain reaction in salivary gland biopsy specimens from patients with Sjogren's syndrome. Am J Med 1991; **90:**286–94.

3 Saito I, Nishimura S, Kudo I, Fox RI, Moro I. Detection of Epstein–Barr virus and human herpes virus type 6 in saliva from patients with lymphoproliferative diseases by the polymerase chain reaction. Arch Oral Biol 1991; **36:**779–84.

4 Fox RI, Pearson G, Vaughan JH. Detection of Epstein–Barr virus-associated antigens and DNA in salivary gland biopsies from patients with Sjogren's syndrome. J Immunol 1986; **137:**3162–8.

5 Fox RI, Bumol T, Fantozzi R, Bone R, Schreiber R. Expression of histocompatibility antigen HLA-DR by salivary gland epithelial cells in Sjogren's syndrome. Arthritis Rheum 1986; **29:**1105–11.

6 Tateishi M, Saito I, Yamamoto K, Miyasaka N. Spontaneous production of Epstein–Barr virus by B lymphoblastoid cell lines obtained from patients with Sjogren's syndrome. Possible involvement of a novel strain of Epstein–Barr virus in disease pathogenesis. Arthritis Rheum 1993; **36:**827–35.

7 Sullivan JL. Epstein–Barr virus and lymphoproliferative disorders. Semin Hematol 1988; **25:**269–79.

8 Inoue N, Harada S, Miyasaka N, Oya A, Yanagi K. Analysis of antibody titers to Epstein–Barr virus nuclear antigens in sera of patients with Sjogren's syndrome and with rheumatoid arthritis. J Infect Dis 1991; **164:**22–8.

9 Yamaoka K, Miyasaka N, Yamamoto K. Possible involvement of Epstein–Barr virus in polyclonal B cell activation in Sjogren's syndrome. Arthritis Rheum 1988; **31:**1014–21.

10 Inoue H, Tsubota K, Ono M et al. Possible involvement of EBV-mediated alpha-fodrin cleavage for organ-specific autoantigen in Sjogren's syndrome. J Immunol 2001; **166:**5801–9.

11 Haneji N, Nakamura T, Takio K et al. Identification of alpha-fodrin as a candidate autoantigen in primary Sjogren's syndrome. Science 1997; **276:**604–7.

12 Rickinson AB, Moss DJ, Wallace LE et al. Long-term T-cell-mediated immunity to Epstein–Barr virus. Cancer Res 1981; **41:**4216–21.

13 Slaughter L, Carson DA, Jensen FC, Holbrook TL, Vaughan JH. In vitro effects of Epstein–Barr virus on peripheral blood mononuclear cells from patients with rheumatoid arthritis and normal subjects. J Exp Med 1978; **148:**1429–34.

14 Countryman J, Miller G. Activation of expression of latent Epstein–Barr herpesvirus after gene transfer with a small cloned subfragment of heterogeneous viral DNA. Proc Natl Acad Sci USA 1985; **82:**4085–9.

15 Rooney CM, Rowe DT, Ragot T, Farrell PJ. The spliced BZLF1 gene of Epstein–Barr virus (EBV) transactivates an early EBV promoter and induces the virus productive cycle. J Virol 1989; **63:**3109–16.

16 zur Hausen H, O'Neill FJ, Freese UK, Hecker E. Persisting oncogenic herpesvirus induced by the tumour promotor TPA. Nature 1978; **272:**373–5.

17 Faggioni A, Zompetta C, Grimaldi S, Barile G, Frati L, Lazdins J. Calcium modulation activates Epstein–Barr virus genome in latently infected cells. Science 1986; **232:**1554–6.

18 Takada K. Cross-linking of cell surface immunoglobulins induces Epstein–Barr virus in Burkitt lymphoma lines. Int J Cancer 1984; **33:**27–32.

19 Luka J, Kallin B, Klein G. Induction of the Epstein–Barr virus (EBV) cycle in latently infected cells by n-butyrate. Virology 1979; **94:**228–31.

20 Meuller-Lantzsch N, Georg B, Yamamoto N, zur Hausen H. Epstein–Barr virus-induced proteins. II. Analysis of surface polypeptides from EBV-producing and -superinfected cells by immunoprecipitation. Virology 1980; **102:**401–11.

21 Mueller-Lantzsch N, Georg B, Yamamoto N, zur Hausen H. Epstein–Barr virus-induced proteins. III. Analysis of polypeptides from P3HR-1-EBV-superinfected NC37 cells by immunoprecipitation. Virology 1980; **102**:231–3.

22 Mannick JB, Asano K, Izumi K, Kieff E, Stamler JS. Nitric oxide produced by human B lymphocytes inhibits apoptosis and Epstein–Barr virus reactivation. Cell 1994; **79**:1137–46.

23 Flamand L, Stefanescu I, Ablashi DV, Menezes J. Activation of the Epstein–Barr virus replicative cycle by human herpesvirus 6. J Virol 1993; **67**:6768–77.

24 di Renzo L, Altiok A, Klein G, Klein E. Endogenous TGF-beta contributes to the induction of the EBV lytic cycle in two Burkitt lymphoma cell lines. Int J Cancer 1994; **57**:914–9.

25 Fox RI, Saito I. Criteria for diagnosis of Sjogren's syndrome. Rheum Dis Clin North Am 1994; **20**:391–407.

26 Yanagawa T, Hayashi Y, Nagamine S, Yoshida H, Yura Y, Sato M. Generation of cells with phenotypes of both intercalated duct-type and myoepithelial cells in human parotid gland adenocarcinoma clonal cells grown in athymic nude mice. Virchows Arch B Cell Pathol Incl Mol Pathol 1986; **51**:187–95.

27 Flemington E, Speck SH. Autoregulation of Epstein–Barr virus putative lytic switch gene BZLF1. J Virol 1990; **64**:1227–32.

28 Flemington E, Speck SH. Identification of phorbol ester response elements in the promoter of Epstein–Barr virus putative lytic switch gene BZLF1. J Virol 1990; **64**:1217–26.

29 Mellinghoff I, Daibata M, Humphreys RE, Mulder C, Takada K, Sairenji T. Early events in Epstein–Barr virus genome expression after activation. regulation by second messengers of B cell activation. Virology 1991; **185**:922–8.

30 Daibata M, Speck SH, Mulder C, Sairenji T. Regulation of the BZLF1 promoter of Epstein–Barr virus by second messengers in anti-immunoglobulin-treated B cells. Virology 1994; **198**:446–54.

31 Fox PC, Grisius MM, Bermudez DK, Sun D. Cytokine mRNA expression in labial salivary glands and cytokine secretion in parotid saliva in Sjogren's syndrome. Adv Exp Med Biol 1998; **438**:909–15.

32 Fox PC, Brennan M, Di Sun P. Cytokine expression in human labial minor salivary gland epithelial cells in health and disease. Arch Oral Biol 1999; **44** (Suppl. 1):S49–52.

33 Fahmi H, Cochet C, Hmama Z, Opolon P, Joab I. Transforming growth factor beta 1 stimulates expression of the Epstein–Barr virus BZLF1 immediate-early gene product ZEBRA by an indirect mechanism which requires the MAPK kinase pathway. J Virol 2000; **74**:5810–8.

34 Morgan DG, Niederman JC, Miller G, Smith HW, Dowaliby JM. Site of Epstein–Barr virus replication in the oropharynx. Lancet 1979; **2**:1154–7.

35 Chang RS, Lewis JP, Abildgaard CF. Prevalence of oropharyngeal excreters of leukocyte-transforming agents among a human population. N Engl J Med 1973; **289**:1325–9.

36 Niller HH, Salamon D, Uhlig J et al. Nucleoprotein structure of immediate-early promoters Zp and Rp and of oriLyt of latent Epstein–Barr virus genomes. J Virol 2002; **76**:4113–8.

37 Farrell PJ, Rowe DT, Rooney CM, Kouzarides T. Epstein–Barr virus BZLF1 trans-activator specifically binds to a consensus AP-1 site and is related to c-fos. EMBO J 1989; **8**:127–32.

38 Shimizu N, Takada K. Analysis of the BZLF1 promoter of Epstein–Barr virus: identification of an anti-immunoglobulin response sequence. J Virol 1993; **67**:3240–5.

39 Daibata M, Mellinghoff I, Takagi S, Humphreys RE, Sairenji T. Effect of genistein, a tyrosine kinase inhibitor, on latent EBV activation induced by cross-linkage of membrane IgG in Akata B cells. J Immunol 1991; **147**:292–7.

40 Liang CL, Chen JL, Hsu YP, Ou JT, Chang YS. Epstein–Barr virus BZLF1 gene is activated by transforming growth factor-beta through cooperativity of Smads and c-Jun/c-Fos proteins. J Biol Chem 2002; **277**:23345–57.

41 Heldin CH, Miyazono K, ten Dijke P. TGF-beta signalling from cell membrane to nucleus through SMAD proteins. Nature 1997; **390**:465–71.

42 Hocevar BA, Brown TL, Howe PH. TGF-beta induces fibronectin synthesis through a c-Jun N-terminal kinase-dependent, Smad4-independent pathway. EMBO J 1999; **18**:1345–56.

43 Wang W, Zhou G, Hu MC, Yao Z, Tan TH. Activation of the hematopoietic progenitor kinase-1 (HPK1)-dependent, stress-activated c-Jun N-terminal kinase (JNK) pathway by transforming growth factor beta (TGF-beta)-activated kinase (TAK1), a kinase mediator of TGF beta signal transduction. J Biol Chem 1997; **272**:22771–5.

44 Hannigan M, Zhan L, Ai Y, Huang CK. The role of p38 MAP kinase in TGF-beta1-induced signal transduction in human neutrophils. Biochem Biophys Res Commun 1998; **246**:55–8.

45 Yamaguchi K, Shirakabe K, Shibuya H et al. Identification of a member of the MAPKKK family as a potential mediator of TGF-beta signal transduction. Science 1995; **270**:2008–11.

46 Davies AH, Grand RJ, Evans FJ, Rickinson AB. Induction of Epstein–Barr virus lytic cycle by tumor-promoting and non-tumor-promoting phorbol esters requires active protein kinase C. J Virol 1991; **65**:6838–44.

47 Halstead J, Kemp K, Ignotz RA. Evidence for involvement of phosphatidylcholine-phospholipase C and protein kinase C in transforming growth factor-beta signaling. J Biol Chem 1995; **270**:13600–3.

48 Suzuki M, Asplund T, Yamashita H, Heldin CH, Heldin P. Stimulation of hyaluronan biosynthesis by platelet-derived growth factor-BB and transforming growth factor-beta 1 involves activation of protein kinase C. Biochem J 1995; **307**:817–21.

49 Fox RI, Kang HI, Ando D, Abrams J, Pisa E. Cytokine mRNA expression in salivary gland biopsies of Sjogren's syndrome. J Immunol 1994; **152**:5532–9.

Ocular Surface Changes With Applanation Contact Lens and Coupling Fluid Use After Argon Laser Photocoagulation in Noninsulin-dependent Diabetes Mellitus

MURAT DOGRU, MD, PhD, BERKANT KADERLI, MD, ONER GELISKEN, MD,
ALI YÜCEL, MD, REMZI AVCI, MD, EIKI GOTO, MD, PhD,
SHIGETO SHIMMURA, MD, PhD, JUN SHIMAZAKI, MD, PhD,
AND KAZUO TSUBOTA, MD, PhD

● PURPOSE: To describe the effect of coupling solutions used during laser photocoagulation on the ocular surface of patients with noninsulin-dependent diabetes mellitus (NIDDM).

● DESIGN: A prospective case-controlled study.

● METHODS: Ninety-two eyes of 46 NIDDM patients with clinically significant macular edema, poor metabolic control of diabetes, and peripheral neuropathy and 100 eyes of 50 normal control subjects were studied. The patients' eyes were assigned to argon green focal/grid laser photocoagulation using an applanation contact lens and one of the coupling fluids; 2% methocel, Thilo-Tears Gel, 1.4% sodium hyaluronate, or 0.9% simple saline. The control subjects received time-matched three-mirror contact lens fundus examinations. All subjects underwent corneal sensitivity measurements, Schirmer test, tear film breakup time, and corneal fluorescein staining before as well as 3 and 8 days after the laser procedures and contact lens examinations. Patients with corneal problems persisting after 8 days were followed longer.

● RESULTS: Diabetic eyes assigned to 2% methocel and 1.4% sodium hyaluronate had significantly lower mean corneal sensitivities and break-up time values as well as significantly higher mean fluorescein staining scores at all examination points after laser photocoagulation. All diabetic eyes with aqueous deficiency assigned to 2% metho-cel and 1.4% sodium hyaluronate developed delayed corneal epithelial healing.

● CONCLUSION: The use of viscous coupling solutions during applanation contact lens–aided laser procedures may be detrimental for the corneal epithelium in poorly controlled NIDDM patients with peripheral neuropathy and coexisting aqueous deficiency. (Am J Ophthalmol 2004;138:381–388. © 2004 by Elsevier Inc. All rights reserved.)

S EVERAL CLINICAL AND EXPERIMENTAL STUDIES HAVE reported structural, metabolic, and functional abnormalities in the conjunctiva and cornea of diabetic patients.[1–6] Schultz and associates[7] reported that 47% to 64% of diabetic patients have primary corneal lesions during their life time. Epithelial fragility, microcystic edema, superficial punctate keratopathy, persistent epithelial defects, recurrent corneal erosions, decreased corneal sensitivity, neurotrophic corneal ulceration, dry eye, filamentary keratitis, and Descemet folds constitute the range of diabetic corneal complications.[8,9] We previously reported that an ocular surface disease existed in patients with noninsulin-dependent diabetes mellitus (NIDDM) characterized by tear film instability, squamous metaplasia, and goblet cell loss, all of which seemed to evolve in close proximity to the status of metabolic control and peripheral neuropathy.[10] Although fundus examinations and laser photocoagulation procedures guided by three-mirror contact lenses and aided by coupling fluid are routinely performed in diabetic patients, the effect of these examinations and procedures on such compromised ocular surfaces remains unclear. Therefore, we performed corneal sensitivity measurements, tear film break-up time analysis, corneal fluorescein stain scoring, and Schirmer tests in NIDDM patients with peripheral neuropathy and poor

© 2004 BY ELSEVIER INC. ALL RIGHTS RESERVED.

control of diabetes who received focal or grid argon laser photocoagulation for clinically significant macular edema and evaluated the ocular surface effects of different coupling solutions used during laser photocoagulation, comparing the results with those of the healthy control subjects.

METHODS

• STUDY POPULATION DETAILS: Ninety-two eyes of 46 patients with NIDDM (21 men, 25 women) aged between 44 and 65 years (mean: 54.9 years) and 100 eyes of 50 healthy subjects (26 men, 24 women) aged from 42 to 67 years (mean: 53.8 years) were recruited. Both groups were similar with regard to age and sex characteristics. Patients with a fasting blood glucose level of greater than 140 mg/dl and Hba1c level of greater than 7.8% were considered to have poor control of their diabetes. The diagnosis of peripheral neuropathy was based on abnormal nerve conduction velocity test results and on the presence of symptoms and signs of diabetic polyneuropathy such as dysesthesias, paresthesias, spontaneous pains, and abnormal deep tendon reflexes. The patients had to have poor control of their diabetes and peripheral neuropathy for inclusion in this study.

Early Treatment of Diabetic Retinopathy Study Criteria were employed to define the stages of diabetic retinopathy using fundus photography and fluorescein angiography. Only those patients with bilateral clinically significant macular edema, which required grid or focal argon laser photocoagulation, were included in this study. Any patient with a secondary systemic disease associated with ischemic fundus changes was excluded from this study. None of the patients had a history of Stevens-Johnson syndrome; chemical, thermal, or radiation injury; or any systemic disorder, nor had any patient undergone an ocular procedure that would create an ocular surface problem. Control subjects had no histories of ocular or systemic disease or of drug or contact lens use.

• INTERVENTIONS AND EXAMINATIONS: All patients underwent argon green focal or grid laser photocoagulation with the Goldman three-mirror contact lens for clinically significant macular edema. None of the patients underwent additional laser applications or applanation contact lens fundus examinations other than the initial examination during their follow-up in this study. The eyes were dilated with 1% tropicamide eyedrops 20 minutes before photocoagulation. The coupling solutions used during photocoagulation were 2% methocel, nonpreserved carbomer gel, 0.9% simple saline, and 1.4% sodium hyaluronate. In this study, 2% methocel and 1.4% sodium hyaluronate were regarded as "viscous," whereas 0.9% simple saline and carbomer gel were referred to as "less viscous" coupling agents. Consecutive diabetic subjects

fulfilling the inclusion criteria were randomly allocated into two age- and sex-matched groups as group I and group II. The right eyes of group I were assigned to 2% methocel coupling solution, and the left eyes were assigned to carbomer gel. Likewise, the right and left eyes of group II were assigned to 0.9% simple saline and 1.4% sodium hyaluronate coupling fluids, respectively. There were 23 patients in each group. The control subjects were also randomly allocated into two age- and sex-matched groups of 25 subjects each (groups III and IV) with the right and the left eyes similarly assigned to the same coupling solutions as for groups I and II. The eyes of the control subjects were also dilated with 1% tropicamide eyedrops 20 minutes before fundus examinations. The control eyes were examined with the three-mirror Goldman lens, time-matched with diabetic eyes. Both the diabetic and the control eyes received a single drop of 0.4% oxybuprocaine chloride topical anesthetic solution 5 minutes before the placement of the applanation contact lens. The laser power settings in patient eyes varied between 50 to 190 mW, and the spot size was 100 to 200 μm. The patients received an average of 100 shots (minimum: 20; maximum: 170 shots). The mean duration of photocoagulation in patients and applanation contact lens examination in the control subjects was 2.7 ± 1.0 minutes (minimum: 1.0 minute; maximum: 5 minutes). The patients and control subjects underwent Schirmer test, corneal sensitivity and break-up time measurements, and corneal fluorescein staining. The effect of the aforementioned coupling solutions on the tear function and ocular surface were observed at 3 days and 8 days after laser photocoagulation in the patients and at the same time points after applanation contact lens fundus examinations in the controls. Corneal sensitivity measurement was also performed at the final visit in diabetic eyes that developed recurrent epithelial disease within 6 months after argon laser photocoagulation. Fluorescein staining was checked 1 hour after the procedures as well. The presence and type of preservatives was recorded for each coupling solution and eyedrop used in this study. Briefly, the 1% tropicamide and 0.4% oxybuprocaine eyedrops contained benzalkonium chloride and polyvinyl alcohol, and the 2% methocel coupling fluid contained benzalkonium chloride as preservatives. All laser procedures and fundus examinations were performed by the same clinician (B.K.). Another researcher who was masked to the patients' data and the data on the type of the coupling fluids performed the tear function and ocular surface examinations at the designated time points (M.D.). The study protocol was approved by the Ethical Board Committee of Uludag University Faculty of Medicine. Informed consent was obtained from patients and the study followed the tenets of the Declaration of Helsinki.

• CORNEAL SENSITIVITY MEASUREMENTS: Measurement of corneal sensitivity was performed using a Cochet-Bonnet aesthesiometer. The mean of five measurements

from central, superior, inferior, nasal, and temporal cornea was recorded as the corneal sensitivity reading of that eye. A corneal sensitivity value less than 50 mm was regarded as low corneal sensitivity.[10-12]

• TEAR FUNCTION EXAMINATIONS: Standard tear film break-up time measurement was performed with fluorescein impregnated strips (Alcon, Ft. Worth, Texas). The interval between the last complete blink and the appearance of the first corneal black spot in the stained tear film was measured three times, and the mean value was calculated. A break-up time value less than 10 seconds was considered abnormal.[13]

For further evaluation of tears, the standard Schirmer test with topical anesthesia (0.4% oxybuprocaine chloride) was performed with standardized strips of filter paper (Alcon). Readings were reported in millimeters of wetting for 5 minutes. A reading of less than 5 mm was referred to as dry eye.[13]

• OCULAR SURFACE STAINING PROCEDURE AND DEFINITIONS: Fluorescein staining of the cornea was carried out after the break-up time measurement and before the Schirmer test. Briefly, the cornea was divided into three equal upper, middle, and lower areas, and the presence of staining by fluorescein was examined. The staining score for each area varied between 0 and 3 points. Fluorescein staining scores ranged between 0 and 9 points.[13,14] A total score greater than 3 points was regarded as abnormal. Any epithelial erosion that had not healed within 8 days after laser photocoagulation was regarded as delayed epithelial healing in this study. Patients with delayed epithelial healing were followed once a month for 6 months to detect further epithelial problems.

• STATISTICAL ANALYSIS: The Mann-Whitney test was used for the analyses of nonparametric values. The analysis of categorized data were performed by the Fisher exact probability test. A probability level less than 5% was considered statistically significant.

RESULTS

• CLINICAL FEATURES: There were no age- or sex-related statistical differences between diabetic and control subjects as well as within groups I and II of diabetic patients and groups III and IV of the control subjects. All patients had nonproliferative diabetic retinopathy with clinically significant macular edema. The mean duration of diabetes was 11.4 ± 4.7 years (minimum: 2 years; maximum: 20 years). The mean fasting blood glucose level was 222.8 ± 80.7 mg/dl (minimum: 143 mg/dl; maximum: 455 mg/dl). All patients had poor control of their diabetes with a mean glycosylated hemoglobin level (HbA1c) of 9.78% (minimum: 7.9%; maximum: 15.2%). All patients had

TABLE 1. Corneal Sensitivity and Tear Function Parameters in Diabetic Patients and Control Subjects

	NIDDM	Control
Corneal sensitivity (mm)	44.3 ± 0.5*	59.3 ± 0.7
BT (sec)	7.8 ± 1.6*	14.4 ± 2.5
Schirmer test (mm)	14.1 ± 10.2	14.3 ± 3.3
Fluorescein score	3.64 ± 0.8*	0.28 ± 0.20

BT = breakup time; NIDDM = noninsulin-dependent diabetes mellitus.
*P < .001 Mann-Whitney test.

peripheral neuropathy and also reported eye fatigue, irritation, burning, and foreign-body sensation. There were no statistically significant differences between patient groups with diabetes (groups I and II) with respect to the duration of diabetes, fasting blood glucose and A1C levels, the status of diabetic retinopathy, and peripheral neuropathy, as well as laser setting parameters including the time of corneal exposure to the three-mirror contact lens. Slit-lamp biomicroscopy did not reveal coexistent blepharitis, meibomian gland disorder, or conjunctivitis in patients or control subjects. Seven NIDDM patients in group I had aqueous deficiency in both eyes. Six patients in group II also had aqueous deficiency in both eyes. Forty-eight eyes with diabetes (52.7%) initially had superficial punctate keratopathy, whereas none of the control subjects had punctate keratopathy.

• CORNEAL SENSITIVITY: All patient eyes initially had low corneal sensitivity. The mean baseline corneal sensitivity in the patients was 44.5 ± 0.5 mm compared with 59.3 ± 0.7 mm in the control subjects (Table 1; P < .05). There were no statistically significant baseline corneal sensitivity differences between right and left eyes within each patient and control group as well as within the right and left eyes of patient groups I and II and control groups III and IV when compared with each other. The mean corneal sensitivity for all diabetic eyes at the eighth day was 41.25 ± 0.5 mm and did not differ from the baseline value (P > .05). However, the mean corneal sensitivity declined significantly in eyes assigned to 2% methocel and 1.4% sodium hyaluronate solutions at the third and eighth days (Figure 1; P<0.05). The mean corneal sensitivity was 42.5 ± 0.5 mm. values did not show any significant differences with respect to the type of coupling solutions in the control subjects as shown in Figure 1 (P > .05). The mean corneal sensitivity was 42.5 ± 0.5 mm in eyes that were assigned to 2% methocel and 1.4% sodium hyaluronate solutions and developed recurrent epithelial disease at their final follow-up.

• TEAR FUNCTION PARAMETERS: There were no statistically significant baseline differences between right and left eyes within each patient and control group as well as
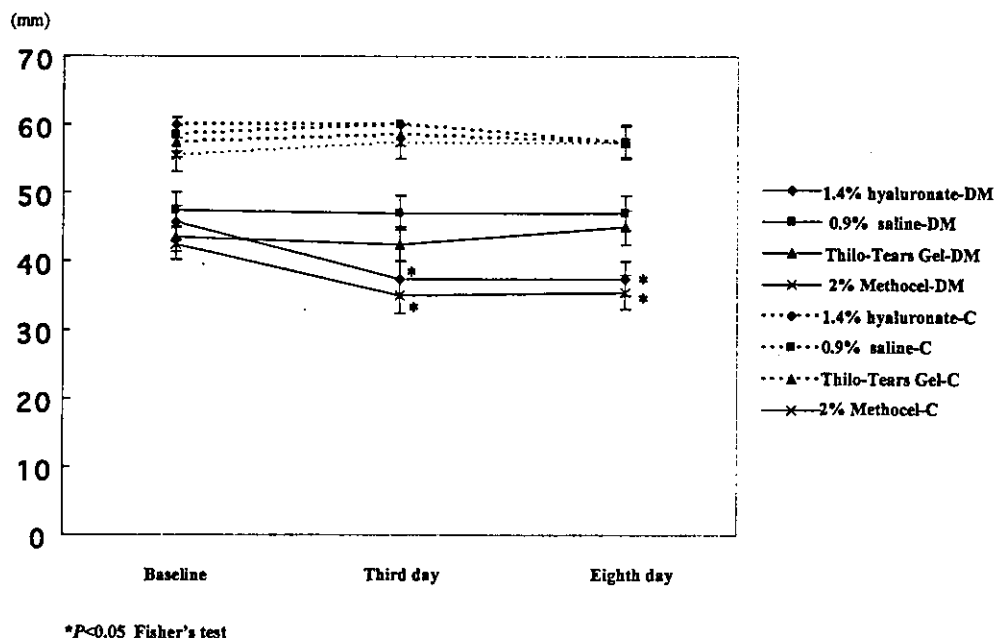
FIGURE 1. Corneal sensitivity changes with different coupling fluids in the control subjects (C) and noninsulin-dependent diabetes mellitus (DM) patients. Note the significant reduction of the mean corneal sensitivity on the third and eighth days compared with baseline in the diabetic eyes assigned to 1.4% sodium hyaluronate and 2% methocel viscous coupling solutions.

within the right and left eyes of patient groups I and II and of control groups III and IV when compared with one another with respect to Schirmer test and break-up time values and the corneal fluorescein staining scores ($P >$ .05). The baseline Schirmer test value averaged 14.1 ± 10.7 mm in patients versus 14.3 ± 3.3 mm in the control subjects ($P >$ .05). There were no significant Schirmer value differences between patient eyes with respect to coupling solution use at any time point (Figure 2). Likewise, no significant changes in the Schirmer test readings were observed in the control eyes with respect to coupling solution use (Figure 2). Of 92 diabetic eyes, 26 (28.2%) had aqueous tear deficiency. Seven of 23 eyes assigned to carbomer gel and their seven fellow eyes assigned to 2% methocel solution in group I were observed to have aqueous-deficient dry eyes. Six of 23 diabetic eyes assigned to 1.4% sodium hyaluronate and their six fellow eyes assigned to 0.9% simple saline solution in group II also had aqueous deficiency.

All diabetic eyes had an initial break-up time value less than 10 seconds. The mean initial breakup time in the patients was 7.8 ± 1.6 seconds compared with 14.4 ± 2.5 seconds in the control subjects (Table 1; $P <$ .05). The mean breakup time significantly decreased in eyes assigned to 2% methocel and 1.4% sodium hyaluronate solutions at the third and eighth days (Figure 3; $P <$ .05). The mean break-up time values did not differ with respect to the type of coupling solutions in the control subjects (Figure 3; $P >$ .05).

• OCULAR SURFACE STAINING: Fifty eyes with diabetes (54.3%) initially had fluorescein staining scores exceeding

3 points, whereas none of the control subjects had superficial punctate keratopathy. The mean baseline fluorescein staining score in the patients was 3.64 ± 0.8 points compared with 0.28 ± 0.20 points in the control subjects (Table 1; $P <$ .05). The mean fluorescein staining score in the patients showed a significant increase in eyes assigned to 2% methocel and 1.4% sodium hyaluronate solutions at the first hour and the third and eighth days (Figure 4; $P <$ .05). The mean staining scores did not show any significant differences with respect to the type of coupling solutions in the control subjects (Figure 4; $P >$ .05). All seven eyes with aqueous deficiency assigned to 2% methocel solution and none of the fellow eyes assigned to carbomer gel in the patients developed delayed epithelial healing after 8 days. Likewise, all six eyes with aqueous deficiency assigned to 1.4% sodium hyaluronate and none of the fellow eyes assigned to 0.9% simple saline solution in the patients developed similar epithelial problems after 8 days. The epithelial defects measured an average of 4.4 mm vertically and 5.8 mm horizontally at their widest diameters. All eyes with epithelial defects showed complete epithelialization and healing initially within 2 weeks upon combined treatment with nonpreserved artificial tear and autologous serum eyedrops and therapeutic contact lenses. However, four aqueous deficient eyes that had been originally assigned to 2% methocel solution in group I and three eyes with aqueous deficiency assigned to 1.4% sodium hyaluronate in group II developed recurrent corneal erosion and neurotrophic ulceration within 6 months. The corneal lesions responded to therapeutic bandage contact lens and

Patients   Controls

P>0.05 Fisher's test
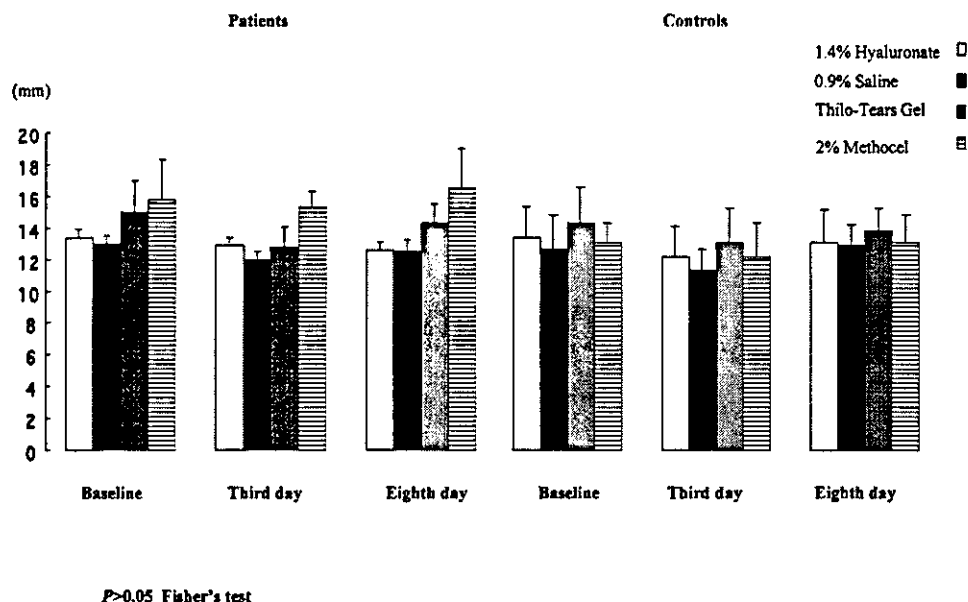
FIGURE 2. Schirmer test changes with different coupling fluids in noninsulin-dependent diabetes mellitus (DM) patients and the control subjects. Note that there were no significant differences between the Schirmer test values in relation to the type of coupling fluids used at a single examination point both in the diabetic and the control eyes. Likewise, time changes in the Schirmer test values on the third and eighth days compared with baseline for each coupling fluid did not show any significance.
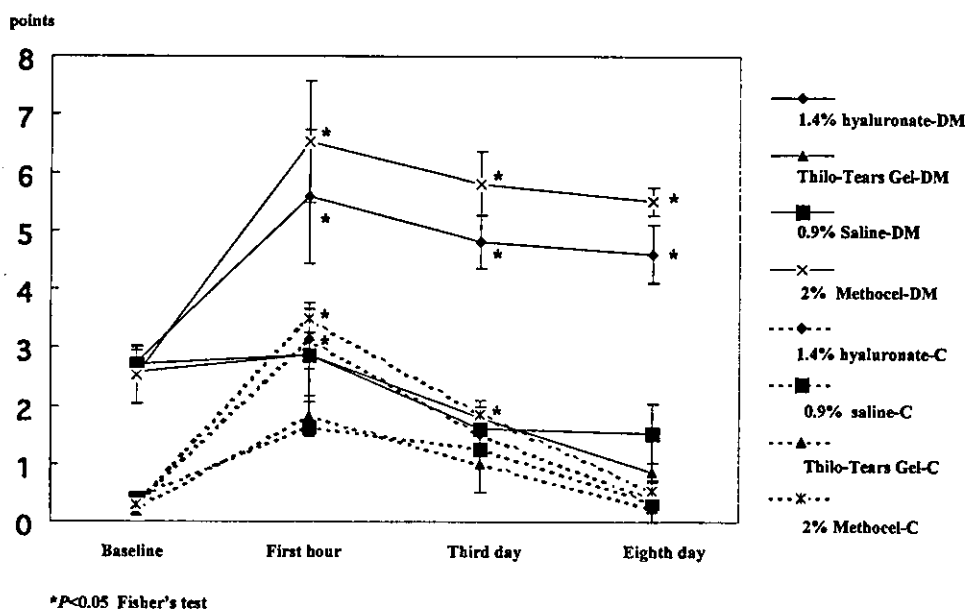

*P<0.05 Fisher's test
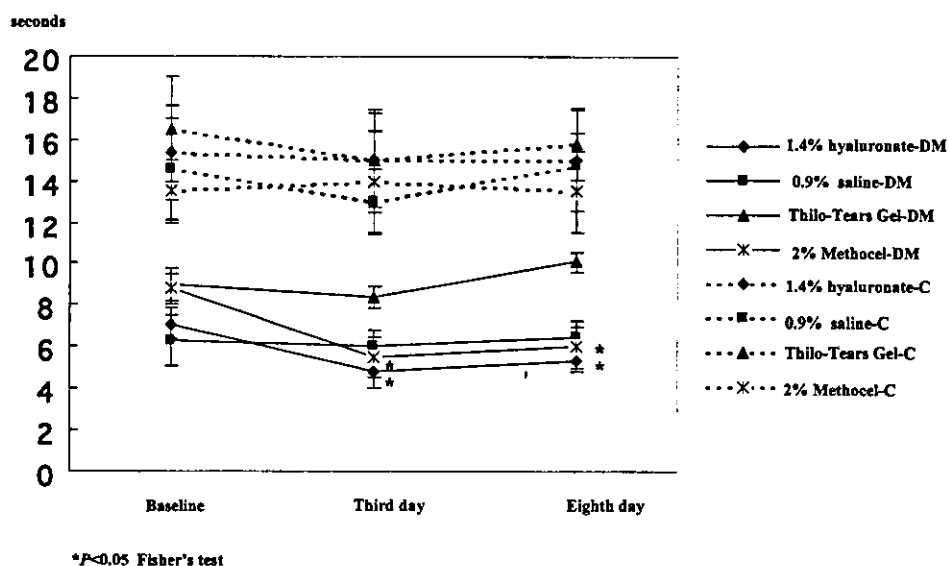
FIGURE 3. Tear film breakup time changes with different coupling fluids in the control subjects (C) and noninsulin-dependent diabetes mellitus (DM) patients. Note the significant reduction of the mean tear film breakup time on the third and eighth days compared with baseline in the diabetic eyes assigned to 1.4% sodium hyaluronate and 2% methocel viscous coupling solutions.

autologous serum eyedrops within 2 months, except in two eyes initially assigned to methocel 2% and one eye initially assigned to 1.4% sodium hyaluronate. These three eyes underwent amniotic membrane transplantation with complete epithelization within 2 weeks. No epithelial problems were observed in the eyes of the control subjects after contact lens fundus examinations.

DISCUSSION

THE CORNEAL EPITHELIUM IS DISEASED IN DIABETIC PATIENTS and exhibits many morphologic changes that can weaken epithelial adherence and impair corneal epithelization.[8,15-20]

FIGURE 4. Corneal fluorescein staining score changes with different coupling fluids in the control subjects (C) and noninsulin-dependent diabetes mellitus (DM) patients. Note the significant increase of the mean fluorescein staining scores on the first hour and the third and eighth days compared with baseline in the diabetic eyes assigned to 1.4% sodium hyaluronate and 2% methocel viscous coupling solutions. The mean staining score also showed a significant increase in the control eyes assigned to 1.4% sodium hyaluronate and 2% methocel viscous coupling solutions the first hour and third day compared with baseline values.

We previously reported that the ocular surface disease in NIDDM was characterized by a disorder of tear quantity and quality, decreased corneal sensitivity, squamous metaplasia, and goblet cell loss, all of which related significantly to poor metabolic control and presence of peripheral neuropathy.[10] Although three-mirror-guided and coupling-fluid-aided fundus examinations and laser photocoagulations are commonly performed on diabetic patients, the effect of these examinations and procedures on such compromised ocular surfaces remains unclear. We found corneal hypoesthesia in all patients, and the mean initial corneal sensitivity was significantly lower than the control subjects in this study. Decreased corneal sensitivity in the patients suggested the presence of corneal epithelial or stromal nerve disease. Indeed, experimental evidence in diabetic animal models points to Schwann cell basal lamina thickening and thinning and axonal degeneration of the unmyelinated corneal nerves. We believe that corneal neuropathy may be a manifestation of the distal peripheral neuropathy of diabetes and may also have resulted from the poor metabolic control in our patients. Changes of intraneural concentration of myoinositols and increased sorbitol levels within the Schwann cell basal lamina leading to mechanical compression or toxic axonal damage have also been shown in corneas of diabetic animal models.[21–23] Corneal sensitivity has also been reported to decrease during phases of hyperglycemia resulting from changes in corneal hydration control.[24]

To our surprise, we found that the mean corneal sensitivity showed a significant reduction on the third and eighth days in the diabetic eyes assigned to viscous coupling solutions, suggesting corneal epithelial or stromal nerve damage probably inflicted by the friction between the viscous agent and the diseased corneal epithelium during the rotational maneuvers of the applanation contact lens. Interestingly, we also observed that eyes with aqueous deficiency assigned to viscous coupling agents developed recurrent epithelial disease, and the mean corneal sensitivity for these eyes at the time of recurrence was still lower than the baseline value. These observations suggest that the recovery of corneal sensitivity seems to be limited in patients with NIDDM who have a poor metabolic control of diabetes and peripheral neuropathy.

Not only corneal sensitivity but also tear function parameters showed marked changes in our patients. All patients complained of dry-eye symptomatology such as eye fatigue, irritation, burning, and foreign-body sensation. All diabetic eyes had breakup-time-deficient dry eyes as described by Lemp,[25] whereas 28.2% of these eyes also had aqueous deficiency. Baseline fluorescein staining score exceeded 3 points in 54.2% of the eyes. These findings strongly suggest that dry eye is a significant feature of the diabetic ocular surface disease. An unexpected finding was that all diabetic eyes with aqueous deficiency assigned to viscous coupling agents during laser photocoagulation developed delayed corneal epithelial healing. Schwartz[26] previously reported that decreased corneal sensitivity alone was not sufficiently reliable to predict the occurrence of corneal abnormalities in diabetic patients undergoing vitrectomy because corneal problems did not develop in all

patients with decreased corneal sensitivity. Our observations suggest that the presence of dry eye acted as a "stress factor" for the development of delayed epithelial healing problems. The preservatives found in the topical mydriatic and anesthetic eyedrops and in the 2% methocel coupling solution might have had a role. The viscous solutions might also have led to a longer exposure of the ocular surface to the preservatives. The failure of reepithelialization in those eyes, once a defect has occurred, might be attributable to the defective cellular adhesion to the underlying basement membrane. The uniformly good response to the use of nonpreserved tears, autologous serum eyedrops, and therapeutic soft contact lenses in our patients supports our belief about the presence of adhesion problems. An ultrastructural study has shown a tendency of diabetic basement membranes to be removed along with basal epithelial cells, whereas nondiabetic epithelial scraping resulted in fracture of basal cells and lesser disruption of the basement membrane (unpublished data; Kenyon and associates, Invest Ophthalmol Vis Sci 1978;17 (suppl): S245). Although we do not have histopathologic evidence, we observed that all aqueous-deficient eyes assigned to viscous coupling agents experienced delayed epithelial healing, and seven of these eyes later developed recurrent epithelial erosion with neurotrophic ulceration. It might be that the greater friction on the ocular surface caused by more viscous agents during rotational maneuvers of the applanation contact lenses inflicts more damage to the basement membranes in aqueous-deficient diabetic eyes. Further ultrastructural evidence is required to support this hypothesis, however. Meticulous attention to the epithelium with therapeutic soft contact lenses, nonpreserved tears, and autologous serum eyedrops nonetheless aided the healing of recurrent corneal epithelial and stromal disease. Amniotic membrane transplantation was observed to be an efficient option achieving rapid epithelialization in those eyes, which remained refractory to the aforementioned treatments for more than 2 months.

The mean exposure time of the diabetic ocular surfaces to the applanation contact lenses in this study was relatively short, ranging between 1 and 5 minutes. The effect of longer and repetitive exposures as in planned panretinal photocoagulations on such compromised ocular surfaces needs to be studied. Serious ocular surface effects are probably less likely in better-controlled diabetic patients without diabetic neuropathy. There is a need for further prospective controlled studies about the effects of laser photocoagulation and applanation contact lens examinations on other subsets of diabetic patients. It should also be noted that the control group in this study mainly served to show the baseline differences of tear functions and ocular surface health from the diabetics and that the control eyes did not undergo a photocoagulation procedure. Although the contact times with the applanation lenses were similar between control and diabetic eyes, the likely degree of

corneal microtrauma, both mechanical and photochemical, probably were not.

The findings of our study may also have applications to vitreoretinal surgery in which contact lenses can be used for prolonged periods during operations. It has been reported that delayed epithelial healing appearing beyond the first week of surgery for diabetic vitreoretinal complications occurred in 43% to 47% of the patients.[27,28] The rate of epithelial debridement and postvitrectomy epithelial problems was found to be higher with infusion contact lenses compared with noncontact lenses.[29] Another study found that the lowest rate of such epithelial problems occurred using "sew-on" contact lenses, in which the surgeon customarily places a cushion of a viscoelastic agent beneath the lens.[30] We would suggest the use of less viscous substances with sew-on lenses based on our observations that call for additional prospective controlled trials.

In conclusion, the use of viscous coupling solutions during applanation contact-lens-aided laser procedures may be detrimental for the corneal epithelium in poorly controlled NIDDM patients with peripheral neuropathy and coexisting aqueous deficiency who need careful follow-up for possible ocular surface problems.

REFERENCES

1. Dabbs CK, Meredith TA. Diabetic eye disease. In: Davidson JK, editor. Clinical diabetes mellitus: a problem oriented approach, 2nd ed. New York: Thieme Medical, 1991:427–443.
2. Tsubota K, Chiba K, Shimazaki J. Corneal epithelium in diabetic patients. Cornea 1991;10:156–160.
3. Shimazaki J, Tsubota K, Yoshida A, et al. Changes of corneal redox state in diabetic animal models. Cornea 1995;14:196–201.
4. Friend J, Ishii Y, Thoft RA. Corneal epithelial changes in diabetic rats. Ophthalmic Res 1982;14:269–278.
5. Chang SW, Hsu HC, Hu FR, Chen MS. Corneal autofluorescence and epithelial barrier function in diabetic patients. Ophthalmic Res 1995;27:74–79.
6. Gobbels M, Spitznas M, Oldendoerp J. Impairment of corneal epithelial barrier function in diabetics. Graefes Arch Clin Exp Ophthalmol 1989;227:142–144.
7. Schultz RO, Van Horn DL, Peters MA, et al. Diabetic keratopathy. Trans Am Ophthalmol Soc 1981;79:180–199.
8. Sanchez-Thorin JC. The cornea in diabetes mellitus. Int Ophthalmol Clin 1998;38:19–36.
9. Goebbels M. Tear secretion and tear film function in insulin dependent diabetics. Br J Ophthalmol 2000;84:19–21.
10. Dogru M, Katakami C, Inoue M. Tear function and ocular surface changes in noninsuline dependent diabetes mellitus. Ophthalmology 2001;108:586–592.
11. Dogru M, Katakami C, Miyashita M, et al. Ocular surface changes after excimer laser phototherapeutic keratectomy. Ophthalmology 2000;107:1144–1152.
12. Dogru M, Yildiz M, Baykara M, et al. Corneal sensitivity and ocular surface changes following preserved amniotic membrane transplantation for nonhealing corneal ulcers. Eye 2003;17:139–148.

13. Leibowitz HM, Villazon S. Corneal procedures. In: Leibowitz HM, Waring GO, editors. Corneal disorders. Philadelphia: WB Saunders, 1998:983–984.
14. Junko H. AD classification of fluorescein staining [in Japanese]. In: Tano Y, Watanabe N, editors. Practical ophthalmology. Tokyo: Bunkodo, 1998:61.
15. Tabatay CA, Bumbacher M, Baumgartner B, Leuenberger PM. Reduced number of hemidesmosomes in the corneal epithelium of diabetics with proliferative vitreoretinopathy. Graefes Arch Clin Exp Ophthalmol 1988;226:389–392.
16. Azar DT, Spurr-Michaud SJ, Tisdale AS, Gipson IK. Decreased penetration of anchoring fibrils into the diabetic stroma. A morphometric analyses. Arch Ophthalmol 1989; 107:1520–1523.
17. Marano CW, Matschinsky FM. Biochemical manifestations of diabetes mellitus in microscopic layers of the cornea and retina. Diabetes Metab Rev 1989;5:1–15.
18. Loy A, Lurie KG, Ghosh A, et al. Diabetes and myoinositol paradox. Diabetes 1990;39:1305–1312.
19. Melato M, Antonutto G, Manconi R, Ponte E. Ocular deposits of immunoglobulin in diabetic retinopathy. Can J Ophthalmol 1982;17:45–46.
20. Tarsio JF, Wigness B, Rhode TD, et al. Nonenzymatic glycation of fibronectin and alterations in molecular associations of cell matrix and basement membrane components in diabetes mellitus. Diabetes 1985;34:477–484.
21. Ishida N, Rao GN, del Cerro M, Aquavella JV. Corneal nerve alterations in diabetes mellitus. Arch Ophthalmol 1984;102:1380–1384.
22. Li J, Mai C, Hu Y. [A study on histochemistry and electron microscopy of corneal nerves in experimental diabetic rabbits (in Chinese with English abstract)]. Zhonghua Yan Ke Za Zhi 1996;32:258–259.
23. Yue DK, Hanwell MA, Satchell PM, Turtle JR. The effect of aldose reductase inhibition on motor nerve conduction velocity in diabetic rats. Diabetes 1982;31:789–794.
24. McNamara NA, Brand RJ, Polse KA, Bourne WM. Corneal function during normal and high serum glucose levels in diabetes. Invest Ophthalmol Vis Sci 1998;39:3–17.
25. Lemp MA. The mucin deficient dry eye. Int Ophthalmol Clin 1973;13:185–189.
26. Schwartz DE. Corneal sensitivity in diabetics. Arch Ophthalmol 1974;91:174–178.
27. Brightbill FS, Myers FL, Bresnick GH. Postvitrectomy keratopathy. Am J Ophthalmol 1978;85:651–655.
28. Foulks GN, Thoft RA, Perry HD, Tolentino FI. Factors related to corneal epithelial complications after closed vitrectomy in diabetics. Arch Ophthalmol 1979;97:1076–1078.
29. Virata SR, Kylstra JA, Singh HT. Corneal epithelial defects following vitrectomy surgery using hand-held, sew-on and non-contact viewing systems. Retina 1999;19:287–290.
30. Friberg TJ, Ohji M, Scherer JJ, Tano Y. Frequency of epithelial debridement during diabetic vitrectomy. Am J Ophthalmol 2003;135:553–554.